nagra.

Technical Report 05-03

Grimsel Test Site
Investigation Phase VI

Pore Space Geometry Project

Characterisation of Pore Space Geometry by ^{14}C-MMA Impregnation

April 2010

M. Kelokaski, M. Siitari-Kauppi, I. Kauppi,
K.-H. Hellmuth, A. Möri, C. Biggin,
W. Kickmaier, L. Inderbitzin and A. Martin

National Cooperative
for the Disposal of
Radioactive Waste

Hardstrasse 73
CH-5430 Wettingen
Switzerland
Tel. +41 56 437 11 11

www.nagra.ch

nagra.

Technical Report 05-03

Grimsel Test Site
Investigation Phase VI

Pore Space Geometry Project

Characterisation of Pore Space Geometry by ^{14}C-MMA Impregnation

April 2010

M. Kelokaski [1], M. Siitari-Kauppi [1], I. Kauppi [1], K.-H. Hellmuth [2], A. Möri [3], C. Biggin [4], W. Kickmaier [4], L. Inderbitzin [3] and A. Martin [4]

[1] Laboratory of Radiochemistry, University of Helsinki, Finland
[2] The Radiation and Nuclear Safety Authority, Finland
[3] Geotechnical Institute, Berne, Switzerland
[4] Nagra, Wettingen, Switzerland

National Cooperative
for the Disposal of
Radioactive Waste

Hardstrasse 73
CH-5430 Wettingen
Switzerland
Tel. +41 56 437 11 11

www.nagra.ch

This report was prepared on behalf of Nagra. The viewpoints presented and conclusions reached are those of the author(s) and do not necessarily represent those of Nagra.

ISSN 1015-2636

Abstract

In Finland high-level radioactive waste is planned to be disposed of in a deep geological repository within a crystalline host rock. The potential role of the geosphere as a safety barrier in repository performance assessment is well established. However uncertainties in both transport pathway definition and pore space characterisation of crystalline rock still exist and the repository safety evaluation today requires going from laboratory and surface-based field work to the underground repository level. Little is known about the changes to rock transport properties during sampling and decompression. Recent investigations using resin impregnation of the rock matrix at the Grimsel Test Site imply that non-conservative errors in calculated transport properties derived from laboratory data may reach factors of two to three.

Due to the potentially great significance of pore space characterisation to safety analysis calculations, it was decided to study the rock matrix characteristics *in situ* using methylmethacrylate (MMA) resin labelled with ^{14}C. During the last decade, the poly-methylmethacrylate (PMMA) method has been developed for characterising the porosity of low permeable granitic rocks in the laboratory. Impregnation with ^{14}C-labelled methylmethacrylate (^{14}C-MMA) and autoradiography allows investigation of the spatial distribution of accessible porosity at the centimetre scale. Quantitative measurements of total or mineral-specific local porosities have been obtained using image analysis tools. Electron microscopy examinations and mercury porosimetry measurements have provided detailed information on pore and fissure apertures.

The objective of this work was to develop an *in situ* application of the PMMA impregnation technique. The changes in rock porosity due to stress relaxation when overcoring the samples from the bedrock for the laboratory studies were examined. The concept behind the work was to inject ^{14}C-MMA from a central borehole at a depth of around 1 metre from the tunnel wall within a 20 cm injection interval. It was assumed that six additional smaller diameter radial boreholes would permit increased drying of the rock matrix and that intrusion of MMA would be observed from the observation boreholes during the injection of the resin. The two main differences between *in situ* and laboratory PMMA impregnations were: 1) drying in situ was done by ventilating warm air whereas in the laboratory, samples were dried by heating in a vacuum; 2) polymerisation in situ was through auto polymerisation whereas in the laboratory polymerisation was achieved by irradiation of the samples.

It was found that air ventilation drying around the injection borehole was not effective enough to dry the rock matrix when ^{14}C-MMA impregnation was applied *in situ.* However the penetration of ^{14}C-MMA into Grimsel granodiorite *in situ* was successful. Autopolymerisation of the resin reduced the amount of impregnation, but the thermal polymerisation succeeded well. The MMA intruded to depths of 2-5 cm from the injection borehole; with maximum penetration along the foliation of the rock texture. The amount of PMMA showed clearly a decreasing trend from injection borehole surface to a depth of 5 cm in the rock matrix.

Zusammenfassung

In Finnland wird geplant, hochradioaktive Abfälle in einem geologischen Tiefenlager in einem kristallinen Wirtgestein zu entsorgen. Die Rolle der Geosphäre als natürliche Barriere in der Sicherheitsanalyse des Lagers ist gut etabliert. Es bestehen aber noch Unsicherheiten bei der Festlegung der Transportpfade sowie bei der Charakterisierung des Porenraums im Kristallingestein. Heutige Sicherheitsanalysen gehen von Labor- und Felduntersuchungen an der Erdoberfläche aus, um die Gegebenheiten auf Lagerniveau zu beschreiben. Über die Veränderungen der Transporteigenschaften des Gesteins infolge der Probenahme und der damit verbundenen Druckentlastung ist relativ wenig bekannt. Jüngste Untersuchungen mit Harzimprägnierung der Gesteinsmatrix im Felslabor Grimsel deuten darauf hin, dass nichtkonservative Fehler in den aus Labordaten berechneten Transporteigenschaften einen Faktor von zwei bis drei erreichen könnten.

Weil die Porenraumcharakterisierung für die in der Sicherheitsanalyse durchgeführten Berechnungen von grosser Bedeutung sein könnte, wurde entschieden, die Eigenschaften der Gesteinsmatrix mit einem MMA-Harz (Methylmethacrylat) markiert mit ^{14}C *in situ* zu untersuchen. Während des letzten Jahrzehnts wurde die PMMA-Methode (Poly-Methylmethacrylat) für die Charakterisierung der Porosität von granitischen Gesteinen mit geringer Durchlässigkeit im Labor entwickelt. Eine Imprägnierung mit Methylmethacrylat markiert mit ^{14}C (^{14}C-MMA) zusammen mit Autoradiographie erlaubt die Ermittlung der räumlichen Verteilung der zugänglichen Porosität auf Zentimeterskala. Quantitative Messungen von der Gesamtporosität oder von mineralspezifischen lokalen Porositäten wurden mit Bildanalysemethoden durchgeführt. Elektronmikroscopie-Untersuchungen und Quecksilberporosimetrie-Messungen haben detaillierte Information über Poren- und Kluftöffnungsweiten geliefert.

Ziel dieser Arbeit war die Entwicklung einer *in situ* Anwendung der PMMA-Imprägnierungsmethode. Die Veränderungen der Gesteinsporosität infolge von Druckentlastung beim Überbohren von Proben für Laborstudien wurden untersucht. Das Versuchskonzept ist wie folgt: aus einem zentralen Bohrloch in einer Tiefe von ca. 1 Meter hinter der Stollenwand wird ^{14}C-MMA in ein Intervall von 20 cm Länge injiziert. Sechs radiale Bohrlöcher mit kleineren Durchmessern erlauben eine erhöhte Austrocknung der Gesteinsmatrix und das Eindringen von MMA während der Harzinjektion wird in Beobachtungsbohrlöchern registriert. Die Hauptunterschiede zwischen PMMA-Imprägnierung *in situ* und im Labor sind wie folgt: 1) die Austrocknung *in situ* erfolgte durch Zirkulation von Warmluft, während die Proben im Labor durch Erwärmung in einem Vakuum getrocknet wurden; 2) *in situ* Polymerisation wurde durch Autopolymerisation und im Labor durch Bestrahlung der Proben erreicht.

Bei der *in situ* Imprägnierung mit ^{14}C-MMA zeigte sich, dass die Luftzirkulation um das Injektionsloch nicht ausreichend war, um die Gesteinsmatrix auszutrocknen. Die *in situ* Penetration von ^{14}C-MMA in den Grimselgranodiorit war aber erfolgreich. Durch die Autopolymerisation des Harzes wurde das Ausmass der Imprägnierung reduziert, die thermische Polymerisation war dagegen erfolgreich. Das MMA konnte bis zu einer Tiefe von 2 bis 5 cm vom Injektionsloch eindringen, mit einer maximalen Eindringung entlang der Schieferung. Es wurde eine deutliche Abnahme von PMMA vom Injektionsloch bis zu einer Tiefe von 5 cm in der Gesteinsmatrix beobachtet.

Résumé

La Finlande prévoit de stocker ses déchets de haute activité dans un dépôt géologique en profondeur aménagé dans une roche cristalline. Le rôle potentiel de la géosphère comme barrière de sûreté est bien établi dans l'analyse de sûreté des dépôts. Il demeure toutefois différentes incertitudes relatives à la définition des structures transmissives et à la caractérisation de l'espace interstitiel dans les roches cristallines. Pour évaluer la sûreté des dépôts géologiques, il convient par conséquent de compléter les recherches effectuées soit en laboratoire, soit sur le terrain à partir de la surface, en passant à la profondeur où seront effectivement aménagées les installations souterraines. On ne sait actuellement pas exactement dans quelle mesure le prélèvement d'échantillons et la décompression affectent les propriétés de transport des roches. Des essais récents au Laboratoire souterrain du Grimsel, où la matrice rocheuse a été imprégnée de résine, indiquent que le coefficient d'erreur dans le calcul des propriétés de transport pourrait atteindre deux à trois par rapport aux données de laboratoire.

Etant donné l'importance potentielle de la caractérisation de l'espace interstitiel pour les calculs de sûreté, il a été décidé d'étudier les caractéristiques de la matrice rocheuse *in situ*, en utilisant de la résine de méthacrylate de méthyle (MMA) marquée au ^{14}C. La méthode au polyméthacrylate de méthyle (PMMA) a été développée au cours de la dernière décennie pour caractériser en laboratoire les roches granitiques peu perméables. L'imprégnation avec du méthacrylate de méthyle marqué au ^{14}C (^{14}C-MMA) et l'autoradiographie permettent d'étudier, à l'échelle du centimètre, la répartition spatiale des pores accessibles. Des mesures quantitatives de la porosité totale ou locale (spécifique à un minéral) ont été effectuées avec des outils d'analyse d'images. Des examens au microscope électronique et des mesures par porosimétrie au mercure ont fourni des informations détaillées sur la distribution et le volume des pores et des fissures.

Ce travail avait pour objectif de mettre au point une application *in situ* de la technique d'imprégnation au PMMA. On a examiné les modifications survenues dans la porosité de la roche en raison du relâchement de la contrainte lors du surcarottage des échantillons de roche pour les études en laboratoire. L'idée à la base de ce travail était d'injecter du ^{14}C-MMA à partir d'un forage central situé à une profondeur d'un mètre environ de la paroi du tunnel, avec un intervalle d'injection de 20 cm. On a posé comme hypothèse que six trous supplémentaires d'un diamètre plus petit favoriseraient le séchage de la matrice rocheuse et que le cheminement du MMA pourrait être observé depuis les forages d'observation pendant l'injection de la résine. Les deux principales différences entre les imprégnations au PMMA *in situ* et en laboratoire étaient les suivantes: 1) Le séchage *in situ* a été effectué par ventilation à l'air chaud, tandis que les échantillons en laboratoire ont été séchés par chauffage sous vide; 2) La polymérisation *in situ* s'est faite par auto-polymérisation, tandis que, en laboratoire, elle a été obtenue par irradiation des échantillons.

On s'est rendu compte que le séchage par ventilation autour du forage d'injection n'était pas assez efficace lorsqu'une imprégnation de la matrice rocheuse au ^{14}C-MMA était effectuée *in situ*. En revanche, la pénétration *in situ* du ^{14}C-MMA dans la granodiorite du Grimsel a réussi. L'autopolymérisation de la résine a réduit le degré d'imprégnation, mais la polymérisation thermique a bien fonctionné. Le MMA a pénétré à des profondeurs de 2 à 5 cm à partir du forage; la pénétration maximale a été observée le long de la texture en feuillets de la roche. La quantité de PMMA a clairement révélé une tendance décroissante entre la surface du trou d'injection et une profondeur de 5 cm dans la matrice rocheuse.

Location of Nagra's underground test facility at the Grimsel Pass in the Central Alps (Bernese Alps) of Switzerland

Grimsel area (view to the west)

1 Grimsel Test Site 2 Lake Raeterichsboden 3 Lake Grimsel 4 Juchlistock

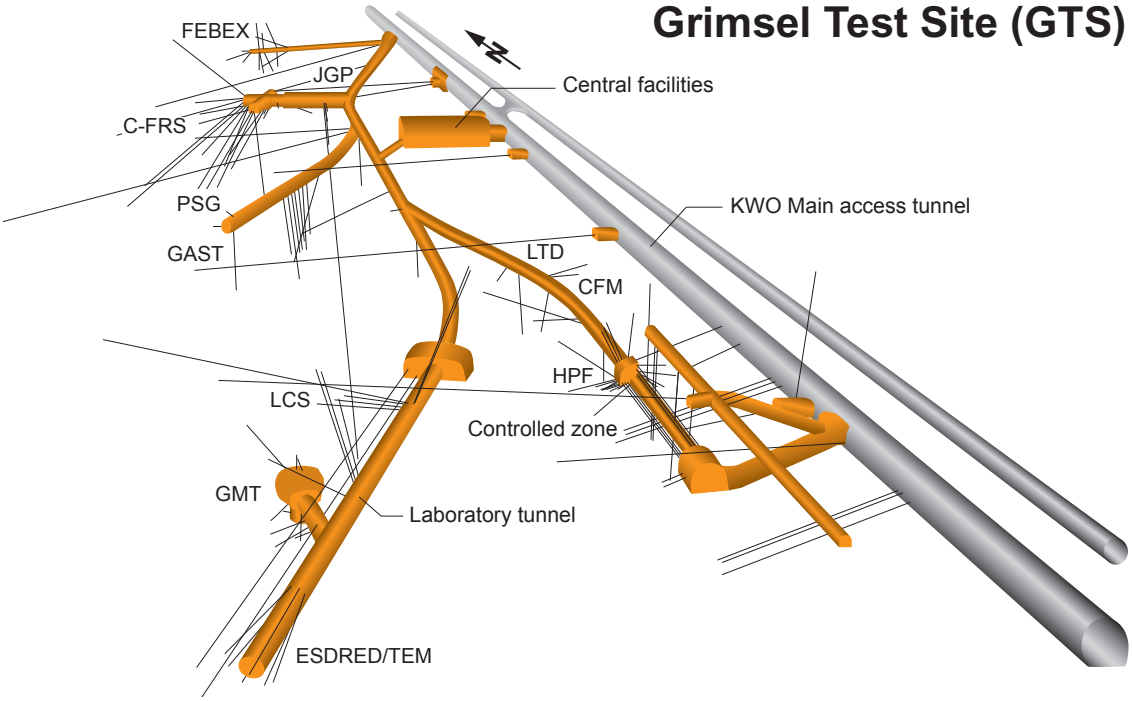

Grimsel Test Site
GTS

KWO-Access tunnel

Laboratory tunnel

Central Aaregranite (CAGR)
High biotite content CAGR

Grimsel-Granodiorite

Shear zone

Lamprophyre

SB — Main investigation borehole

ZB — Central facilities

GTS Phase VI 2003-2013

CFM — Colloid Formation and Migration

C-FRS — Criepi Fractured Rock Studies

ESDRED/TEM — Test and Evaluation of Monitoring Systems

FEBEX — Full-scale Engineered Barriers Experiment

GAST — Gas-permeable Seal Test

GMT — Gas Migration Test in the EBS

HPF — Hyperalkaline Plume

JGP — JAEA Grouting Project

LCS — Long-Term Cement Studies

LTD — Long Term Diffusion

PSG — Pore Space Geometry

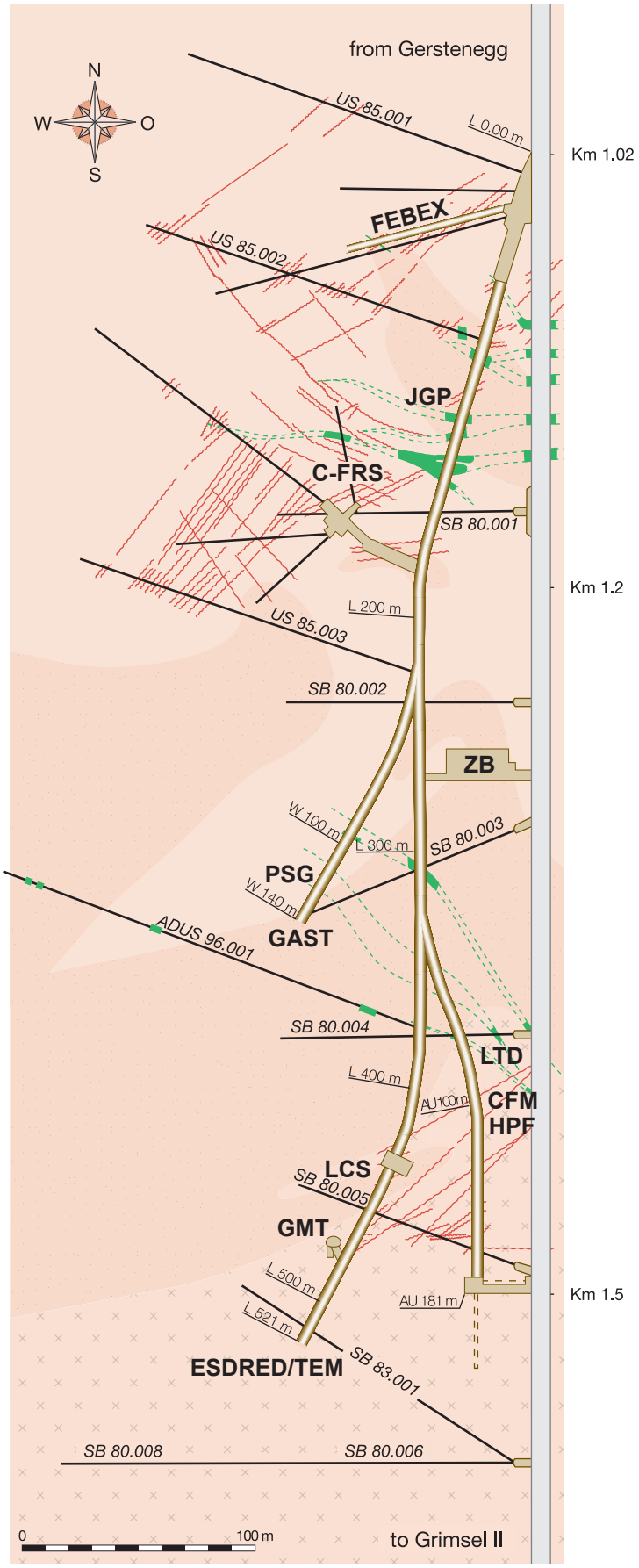

Table of Contents

List of Tables

List of Figures

1 Introduction

1.1 Background

In Finland, as in many other countries, high-level radioactive waste is planned to be disposed of in a deep geological repository within a crystalline host rock. The potential role of the geosphere as a safety barrier in repository performance assessment is well known. However the uncertainties in both transport pathway definition and pore space characterisation of crystalline rock exist and the repository safety evaluation requires going from laboratory and surface-based field work to the underground repository level. Little is known about the changes to rock transport properties during sampling and decompression. Recent investigations using resin impregnation of the rock matrix at the Grimsel Test Site (GTS) imply that non-conservative errors in calculated transport properties derived from laboratory data may reach factors of two to three. This may lead to overestimates of the rock diffusivity and rock porosity, leading to an overestimation of matrix diffusion which is, in turn, non-conservative in the performance assessment (PA) sense as it leads to an apparently greater degree of radionuclide immobilisation in the far field (McKinley, 1989).

Due to the potentially great significance of pore space characterisation to safety analysis calculations, it was decided to study the rock matrix characteristics *in situ* using an alternative resin technique to that previously tested NHC-9 acrylic liquid in the Connected Porosity project (CP) carried out at the GTS (Möri et al. 2003). As an alternative resin technique methyl-methacrylate (MMA) resin labelled with ^{14}C was chosen for *in situ* tests. The main difference between the two acrylic resins is that NHC-9 is soluble in water whereas ^{14}C-MMA is almost insoluble. During the last decade, the poly-methylmethacrylate (PMMA) method has been developed for characterising the porosity of low permeable granitic rocks in the laboratory (Hellmuth et al. 1993, 1994 and Siitari-Kauppi, 2002). Impregnation with ^{14}C-labelled methyl-methacrylate (^{14}C-MMA) and autoradiography allows investigation of the spatial distribution of accessible porosity at the centimetre scale. Quantitative measurements of total or mineral-specific local porosities can be obtained using image analysis tools and electron microscopy examinations and mercury porosimetry measurements have provided detailed information of pore and fissure apertures.

1.2 Objective

The objective of the Pore Space Geometry project (PSG) was to develop an *in situ* application of the PMMA impregnation technique. The work comprises the results of porosity measurements on Grimsel Granodiorite in the laboratory and *in situ* by the ^{14}C-MMA autoradiography method. The different post mortem analyses of the ^{14}C-MMA impregnated samples were executed to find out if there is a difference in porosity on laboratory versus *in situ scales*. The interpretation should reveal if there are important changes in rock porosity for example due to the stress relaxation when boring the samples from the bedrock for the laboratory studies compared to the real *in situ* situation.

1.3 Concept

The concept behind the work was to inject ^{14}C-MMA from a central borehole at a depth of around one metre from the tunnel wall within a 20 cm injection interval. A further six smaller diameter radial observation boreholes permits increased drying of the rock matrix. A schematic of the experimental layout is shown in Fig. 1. Fig. 2 shows (1) the experiments carried out with the core obtained when drilling the injection borehole, (2) activities carried out *in situ* and (3) the laboratory experiments carried out on the overcore from the *in situ* experiment.

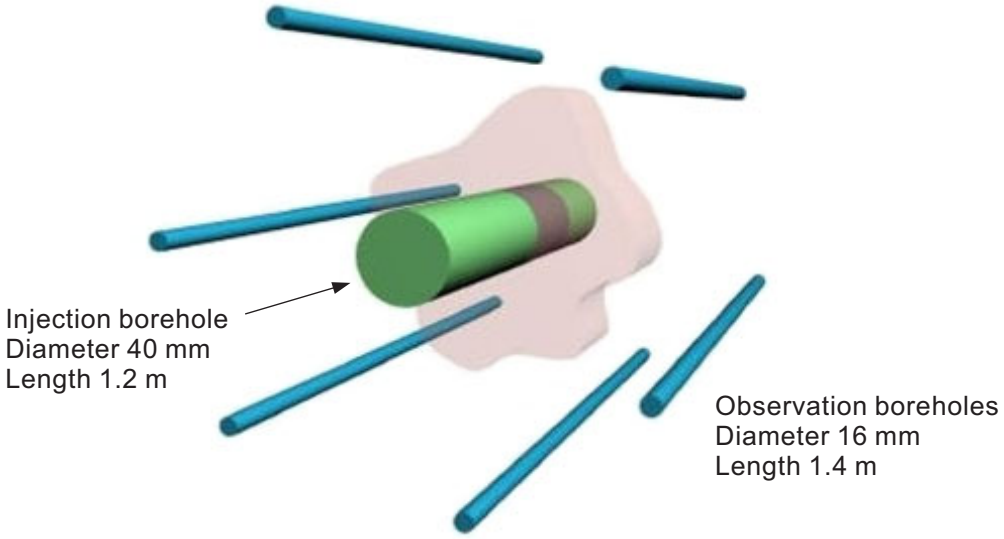

Fig. 1: Schematic layout of the PSG experiment

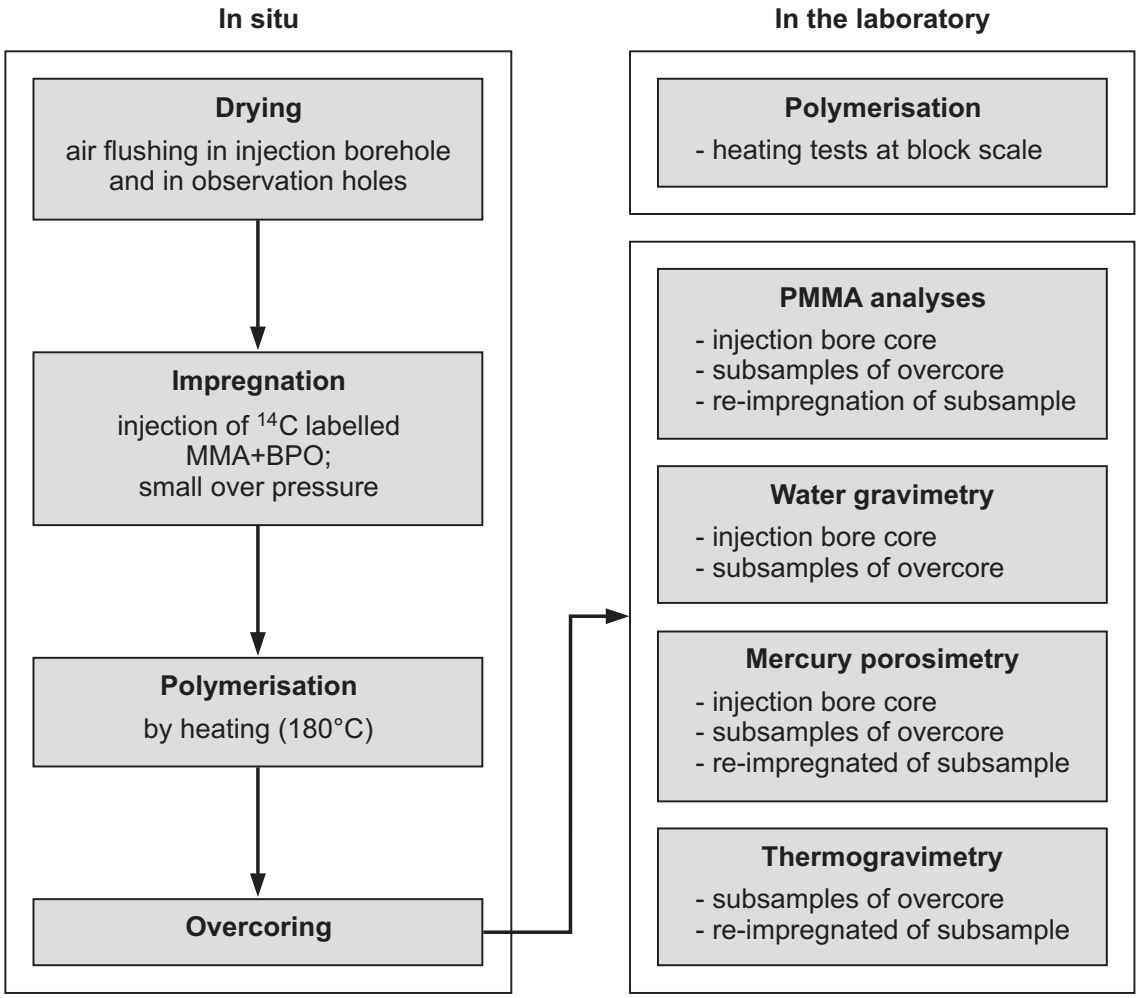

Fig. 2: Diagram showing steps in *in situ* impregnation and porosity analyses in the laboratory

2 Materials and methods in the laboratory

The overall differences between the laboratory ^{14}C-MMA impregnation and the *in situ* ^{14}C-MMA impregnation are listed here. Laboratory ^{14}C-MMA impregnation of the matrix pore space takes place in five distinct steps (Siitari-Kauppi 2002, Sardini 2006):

Step 1. drying of the centimetre scale rock samples in a vacuum in aluminium chambers

Step 2. impregnation with ^{14}C or ^{3}H labelled methylmethacrylate in aluminium chambers in initial vacuum of 10 Pa

Step 3. polymerisation with a ^{60}Co source or with heat

Step 4. autoradiography of the impregnated rock sample

Step 5. digital image analysis of autoradiographs

When working *in situ* in the geological environment, changes have to be adopted. Drying and impregnation can not be done in a vacuum and irradiation polymerisation is not possible. The PMMA technique was studied extensively to further develop the technique to allow its application in the geological environment. The *in situ* project was broken down into a series of stages:

Step 1. drying the rock matrix by air flushing

Step 2. impregnation with ^{14}C labelled methylmethacrylate + bentsoylperoxide (1 g (BPO/100 ml MMA)

Step 3. polymerisation by heating the rock matrix from the injection borehole

Step 4. overcoring

Step 5. autoradiography of the impregnated rock sample

Step 6. digital image analysis of autoradiographs

The *in situ* test site at GTS situated in the non controlled zone and the radioactivity of the ^{14}C-MMA was kept under the exemption limit.

2.1 Drilling and sampling of boreholes in January 2004

The PSG experiment had two criteria regarding site selection for the *in situ* experiment:

- The in-situ experiment should be located in homogenous rock matrix
- It should be possible to dry the rock matrix prior to injection of resin

After a detailed evaluation of several potential locations within the GTS it was suggested that TM 131 in the WT tunnel would provide a suitable location for the PSG project. The rock in this area represents the weakly schistose central Aare Granite. In order to investigate this potential experimental location, a borehole was drilled to allow the core material to be examined in detail in the laboratory. If successful this borehole would act as the central injection hole for the experiment.

Drilling was performed by GTS staff using a single core barrel Hilti drilling machine. The borehole length was 1.27 m and a diameter of 40 mm. The borehole was named BO PSG 04.001.

Fig. 3: Drill core from 0 to 0.28 m. The arrow indicates the tunnel wall surface

Fig. 4: Drill core from 0.28 m to 0.58 m

Fig. 5: Drill core from 0.53 m to 0.83 m

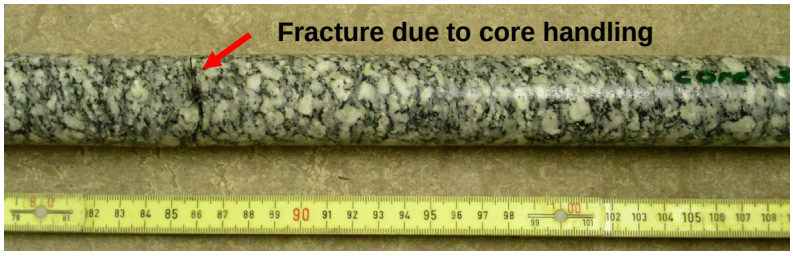

Fig. 6: Drill core from 0.79 m to 1.08 m

Fig. 7: Drill core from 0.99 m to 1.27 m

The drill core, named IHC, was analysed using the PMMA technique, water gravimetry, mercury porosimetry and thermogravimetry in the laboratory. The drillcore length was 1.27 m and diameter 35 mm (the difference between the core diameter and the borehole diameter represents the material lost during the drilling procedure). Due to the drilling equipment the core had to be broken into three pieces (0.00 – 0.52 m, 0.52 – 0.85 m and 0.85 – 1.27 m). Photographs of the drill core sections are shown in Figs. 3 to 7.

The geological examination of the drill core IHC showed no evidence of structural inhomogeneities. For further evidence of the homogeneity of this site, the borehole walls were also examined. Examination of the borehole was performed with two different instruments (see Fig. 8):

- The wall of the borehole was optically observed using a small mirror which was attached to a 1.50 m long aluminium profile in a 45 ° angle.
- The borehole surface was also tested using a metal needle.

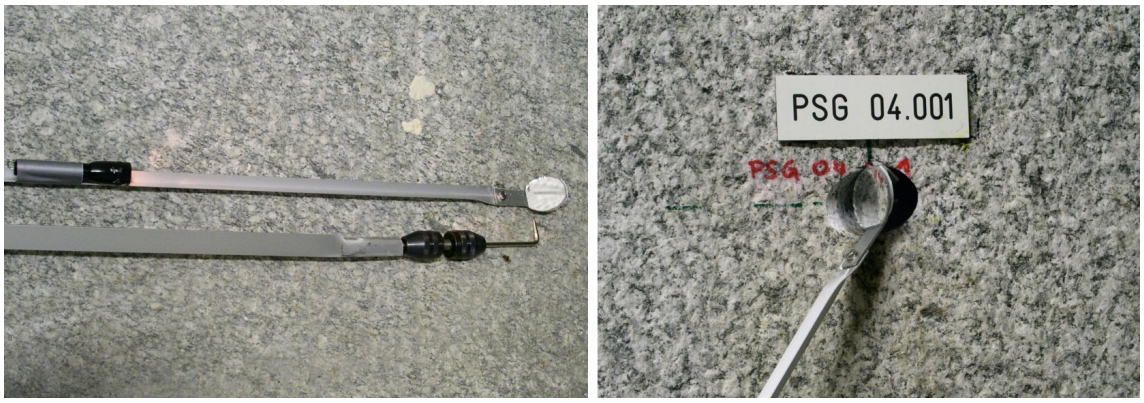

Fig. 8: The left picture shows the two instruments used to examine the borehole. The right picture shows the mirror instrument just inside the PSG borehole

The examination of the borehole showed no evidence for structural inhomogeneities and was therefore suitable for the *in situ* PSG experiment. The six observation boreholes (∅ = 16 mm) were then drilled around the central borehole with a 15 cm radius from the central borehole. Additionally, three boreholes were drilled to allow a test of the heating equipment, which would later be used to polymerise the resin *in situ* (Section 2.3). A summary of the PSG boreholes can be found in Tab. 1 and the layout of the PSG *in situ* impregnation test site is shown in Fig. 9.

The core from the central injection borehole was sent to the University of Helsinki for a series of different laboratory experiments on the excavated sample. The aim of these experiments was to provide identical material to the *in situ* test area to permit a comparison of laboratory and *in situ* data.

Tab. 1: PSG borehole data

Borehole name	**Date of drilling**	**Length** (cm)	**Diameter** (mm)	**Azimuth** (°)	**Dip** (°)	**Purpose**
PSG 04.001	28/01/04	126	40	340	-8	Resin injection borehole
PSG 04.002	2/02/04	138	40	340	-8	Heater test "injection" borehole
PSG 04.003	2/02/04	139.5	16	340	-8	Heater test 7.5 cm from central hole
PSG 04.004	2/02/04	140	16	340	-8	Heater test 15 cm from central hole
PSG 04.005	30/01/04	139.5	16	340	-8	Heater test 30 cm from central hole and Ventilation/ observation borehole in main in-situ test
PSG 04.006	30/01/04	140	16	340	-8	Ventilation/observation borehole in main in-situ test
PSG 04.007	30/01/04	139.5	16	340	-8	Ventilation/observation borehole in main in-situ test
PSG 04.008	30/01/04	140	16	340	-8	Ventilation/observation borehole in main in-situ test
PSG 04.009	30/01/04	139.5	16	340	-8	Ventilation/observation borehole in main in-situ test
PSG 04.010	30/01/04	139.5	16	340	-8	Ventilation/observation borehole in main in-situ test
PSG 04.011	2/02/04	25	40	0	-90	Resin test borehole on opposite side of tunnel.

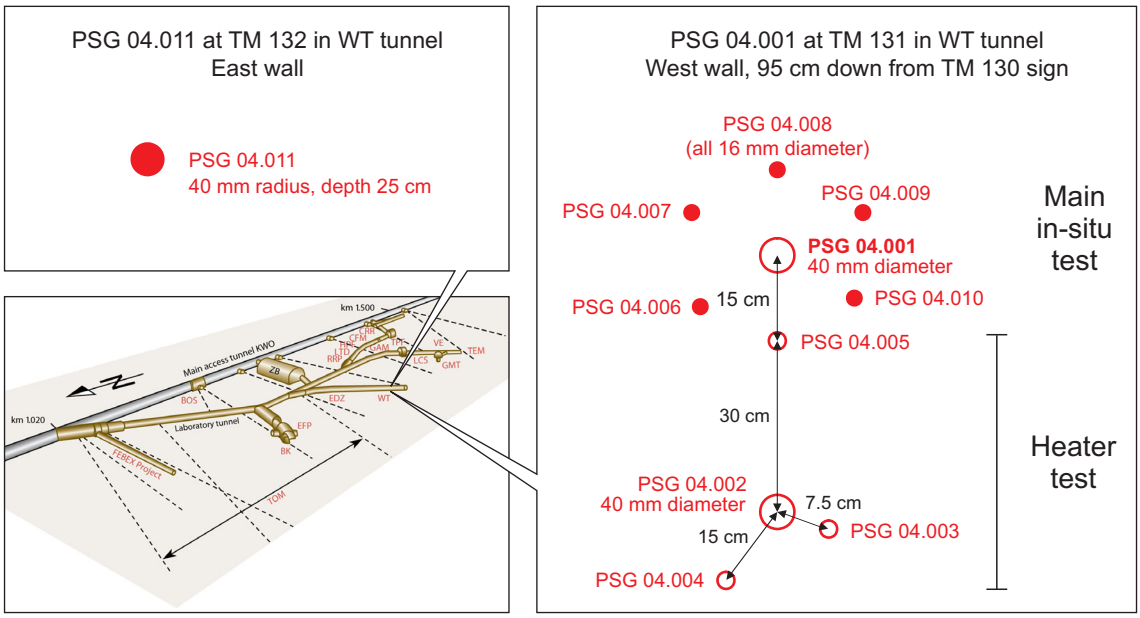

Fig. 9: Layout of the Pore Space Geometry (PSG) boreholes in the WT tunnel of the Grimsel Test Site, February 2004

2.2 The PMMA technique

Properties of methylmethacrylate

The ^{14}C-MMA porosity measurement technique is presented in Hellmuth et al. 1993, 1994, Siitari-Kauppi et al. 1998, Siitari-Kauppi 2002 and Sardini et al. 2006. The method is based on the impregnation of the rock volume with liquid monomeric ^{14}C-labelled methylmethacrylate (MMA). The MMA molecule was selected because of its physico-chemical properties:

1. at 20° C, the dynamic viscosity of the MMA molecule is low (0.584 mPas) compared to the viscosity of water (1.005 mPas)
2. the MMA molecule is a small organic molecule (100.1 g/mol) having thickness of approximately 0.4 nm and a length of approximately 1 nm, whereas the diameter of a water molecule is 0.193 nm
3. the MMA molecule is a good wetting agent for the negatively charged silicate surfaces because of its high permanent dipole moment

Since the MMA molecule is strongly hydrophobic, samples must be dried before impregnation to remove any free water from the connected void space. One of the disadvantages of the PMMA technique compared to other resin techniques is that the MMA monomer cannot displace water from the pore space within the rock. Saturated ground water conditions will inhibit the injection and it is therefore necessary to dry the rock matrix prior to the injection. Tab. 2 lists the viscosities of the different epoxy and acrylic resins (Frieg et al. 1998) as well as the viscosity of water.

Tab. 2: List of different types of resins' viscosities

resin	**viscosity Pa s**
MMA	0.00584 (20 °C)
water	0.00895 (25 °C)
monomer of acrylic resin	≈ 0.03 (5 ° C), < 0.01(20 ° C)
monomer of epoxy resin components	0.15 (13 ° C), 0.1 (23 ° C)

Tab. 3 compares the properties of acrylic resins ^{14}C-MMA and recently used NHC-9 (Möri et al. 2003). NHC-9 has been used in *in situ* impregnation at GTS since the mid 90's. Two main differences are the miscibility with water and the detection of the resin when it stays within the pore voids. The ^{14}C-MMA is not miscible with water whereas NHC-9 is. The polymerized NHC-9 is detected by its fluorescence emission due to the eosine dye added to the liquid. ^{14}C-MMA detection is based on autoradiography.

Tab. 3: Properties of acrylic resins ^{14}C-MMA and NHC-9

	^{14}C-MMA acrylic resin	**NHC-9 acrylic resin**
Material basis	^{14}C labelled methylmethacrylate + fluorescent dye + BPO as initiator for heating polymerization	Single component acrylate + fluorescent dye + initiator
Polymerisation	By heat (>40°)	By heat (>40°)
Density ($kgcm^{-3}$) 20 °C	1180	1070
Boiling point (°C)	100.2	>100
Melting point (°C)	-48	<-10
Storage stability	Several years if 100 ppm hydrochinone is added as stabilizer	6 months

Drying, impregnation and irradiation polymerization

The samples are dried at temperatures ranging from 80 – 105° C. These conditions yield a good compromise with a reasonably short drying time (1 – 3 weeks) and negligible damage of the material. The cores were then impregnated with ^{14}C labelled MMA solution in a vacuum (10 Pa), resulting in a homogeneous concentration of ^{14}C throughout the connected porosity. The ^{14}C-MMA in the sample was then polymerized with a ^{60}Co gamma source. Polymethyl-methacrylate (PMMA) is formed by free radical vinyl polymerisation of the MMA monomer:

$$CH_2=C(CH_3)CO_2CH_3 >> -(CH_2-C(CH_3)CO_2CH_3)-$$

During gamma ray exposure, the samples were immersed into MMA saturated water to avoid excessive heating. A total dose of 50 – 60 kGy was sufficient for complete bulk MMA polymerization. Excited states in the crystals of certain minerals, due to high-energy irradiation, were slowly released at room temperature and the resulting optical luminescence may have caused an unwanted blackening of the autoradiographic film (Pinnioja et al. 1999). This luminescence radiation was released before exposure of the film by heating the samples to 120° C for 3 hours before sawing into slices for autoradiography.

Autoradiography and porosity calculation

The sawn and polished rock slices were placed on an autoradiographic film alongside a ^{14}C-MMA calibration series. The rock surfaces were exposed on Kodak BioMax MR film, a high-performance autoradiographic film for ^{14}C and other low-energy β-emitting nuclides. The nominal resolution of the β film is a few μm. The final spatial resolution achieved depends on the roughness of the sawn surface, the space between the rock and autoradiographic film and the range of the 155 keV beta particles in the rock matrix. The spatial resolution of the autoradiographic film is defined as the half-width of the measured optical density across a particular feature of the rock; for ^{14}C, the resolution is 20 μm.

The monomer used was ^{14}C-MMA with a specific activity of 2 – 5 mCi/g, a total activity of 50 mCi, and a radiochemical purity of >95 %. In this study, the dilution of the tracer varied between 555,000 Bq/ml and 222,000 Bq/ml. The calibration sources were prepared by diluting the ^{14}C-MMA with inactive MMA. Activities ranged from 462 Bq/ml to 185,000 Bq/ml. With this level of tracer activity and the type of autoradiographic film employed, the exposure times

for samples ranged from three days to four weeks. While the short exposure time is convenient for the quantitative determination of porosity, the long exposure time is better for the qualitative determination of micro-fracturing. The visible features on the autoradiograph result from the beta emissions of the ^{14}C-MMA impregnated rock surfaces and show a 2D cross-section of the 3D connected pore space of the sample.

Interpretation of the results is based on digital image analysis of the autoradiographs. Digital image analysis started by dividing the autoradiograph into area units called pixels. In this study, the 600 dpi (dots per square inch) resolution used in the quantitative analysis resulted in a pixel size of (42.5 × 42.5) μm^2. Essentially, all the intensities of the sub domains were converted into corresponding optical densities, and these were in turn converted into levels of activity with the help of the calibration curves measured for each exposure. Finally, the levels of activity were converted into their corresponding porosities. In principle, the interpretation is based on studying the abundance of tracer in each sub-domain. Hellmuth et al. (1993) contains the basic calculations related to porosity determination. The software program Mankeli was used in this study, implemented using the Matlab Image Processing Toolbox.

The amount of tracer in the sample, and the volumetric porosity, can be derived from the blackening of the film caused by the radiation emitted from the plane surface of the rock section. If the pore sizes are well below the resolution of the autoradiography, the major fraction of the beta radiation emitted is attenuated by silicate. The tracer can thus be considered to be diluted by silicate. For the ^{14}C-MMA method, the bulk density must be known, there must be only two phases (i.e. mineral and PMMA), and the pores and minerals must be homogeneously distributed below the lateral resolution limit of the autoradiography. Fig. 10 shows an example of ^{14}C-MMA autoradiograph of a Finnish granite.

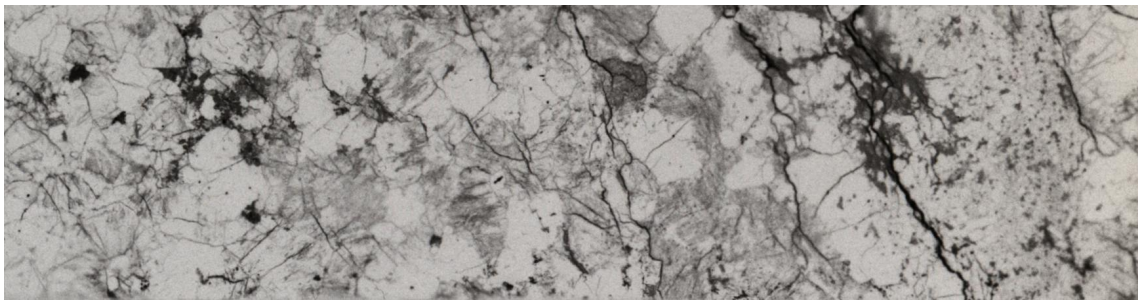

Fig. 10: A ^{14}C-MMA autoradiograph showing different porous regions from dark grey to nonporous regions with light areas. (Width of sample is 8 cm)

The PMMA procedure for Injection Hole Core samples in the laboratory

The Injection Hole Core (IHC) was produced during drilling of the PSG 04.001 in January 2004. Rock cores shown in Fig. 3 to 7 were sent to HYRL for PMMA impregnations in the laboratory. Three samples of IHC were impregnated with ^{14}C-MMA. One sample with high ^{14}C activity and two samples with low activity; for a FLA 5100 (Fuji) scanner tests. The FLA scanner technique replaces the slow conventional film autoradiography. The sensitivity of the FLA scanner to detect the spatial radioactivity from rock samples is 50 – 100 times better than the X ray films' sensitivity (Kämäräinen et al. 2006). The activities applied for the IHC samples were 888 kBq/ml and 37 kBq/ml. The MMA solutions of low activity were doped with fluorecein dyes, Epodye and Bluedye.

The PMMA technique conditions for the three samples were:.1) ICH 5 – 85 cm drying for six days in a vacuum, max. temperature 100° C, impregnation over 20 days in a vacuum, irradiation polymerisation using total dose of 65 kGy (dose rate 0.45 kGy/h), 2) ICH 71 – 75 cm and IHC 67 – 71 cm, drying for five days in a vacuum, max temperature 100° C, impregnation over 15 days in a vacuum, irradiation polymerisation using total dose of 55 kGy, fluorescence Blue (Knorring) and Epodye (Struers) dyes.

Fig. 11: Impregnation was performed in vacuum chambers with an initial vacuum of 10 Pa. (Siitari-Kauppi 2002)

2.3 Water saturation gravimetry, mercury porosimetry and chemical porosity analyses

The porosities of the non impregnated, PMMA impregnated in the laboratory and PMMA *in situ* impregnated samples were analysed by conventional porosity measurement techniques such as water gravimetry, mercury porosimetry and thermo gravimetry i.e. chemical porosimetry method Möri et al. 2003).

Five samples were taken for water saturation gravimetry measurements. Samples were 2 to 4 cm in height and 3.5 cm in diameter. Samples are coded IHC3-6 cm, IHC6-9 cm, IHC9-12 cm, IHC56-59 cm and IHC59-63 cm. E_{H2O} and D_{H2O} samples from the 04.001-OverCore D and E were also analysed by water saturation gravimetry.

Mercury porosimetry was performed on 04.001-OC overcored subsamples; Ef 1 and 2 samples representing non impregnated samples (taken from the outer zone of 04.001-OC-E), Df 1 and 2 representing laboratory impregnated samples (taken from the outer zone of 04.001-OC-D-reimpregnated), Ec 1 and 2 representing *in situ* impregnated samples (taken next to the injection borehole surface of the sub-sample 04.001-OC-E) and finally Dc 1 and 2 representing *in situ*+laboratory impregnated samples (taken next to the injection borehole surface of the sub-sample 04.001-OC-D-reimpregnated). The mercury porosimetry analyses were performed by Dr. P. Klobes from Bundesanstalt für Materialforschung und -prüfung (BAM), Germany.

The samples for chemical porosity analyses i.e. thermo gravimetry (Kauppi 2007) were crushed rock samples from the rock slices of sub samples 04.001-OC E and 04.001-OC-D-ri. Fig. 12 illustrates the cutting scheme for the rock slices. The porosity profile Etga represents the *in situ* impregnation results. Dtga 2/A shows the *in situ* and laboratory impregnated sample and the sample Dtga 1/A shows the laboratory impregnated sample.

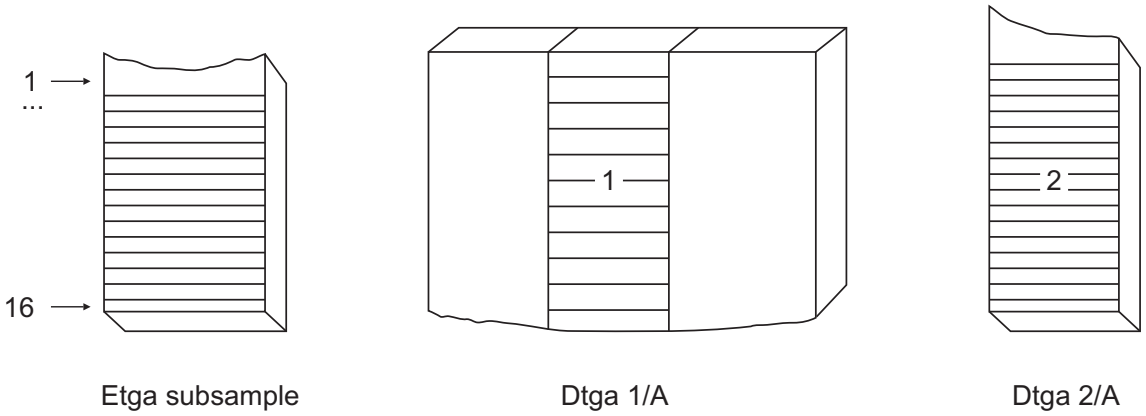

Fig. 12: Partition diagrams for chemical porosity analyses by thermo gravimetry for sub-samples 04.001-OC-E and 04.001-OC-D (see Fig. 28)

3 Initial tests for *in situ* impregnation

3.1 "Pot life" tests for MMA

Tests in the laboratory

The methylmethacrylate (Merck) contains 100 ppm hydrochinone to avoid possible autopolymerisation during storage at the liquid in a freezer, fridge or in the laboratory (about 20° C). However the resin pot life experiments were performed to test the stability of ^{14}C-MMA in the laboratory. Resin was placed in an aluminium chamber in a vacuum for 2.5 months. Another test was done in a stainless steel pressure vial, where the resin was kept for 1.5 months under 5 bar overpressure in a nitrogen atmosphere. In both tests MMA was viscous and autopolymerisation of the resin did not occur.

Test at GTS

A pot life test was performed at the GTS where the temperature is 13 – 14° C. The borehole PSG 04.011 was drilled for this test. It is located at TM 132 in the WT tunnel on the East wall. This borehole (depth 25 cm and diameter of 4 cm) was filled with 200 ml of inactive MMA with 2.5 g of bentsoyl peroxide (BPO) in May 2004. In addition, fluorescence dye (EpoDye, Sruers) was added to the solution. The pot life and the behaviour of the *in situ* resin were determined without applying an injection overpressure. The level of the resin in the borehole was recorded weekly. The resin remained liquid for several months under *in situ* conditions. It was assumed that the resin would remain in the borehole but infiltration into the "wet", partly saturated rock took place.

In December 2005, it was observed that the resin had polymerized and an overcore of 14 cm in diameter (PSG 04.011-OC) was taken (Fig. 13a). Polymerized MMA was found on the bottom of the borehole. UV light revealed fluorescence in the rock matrix up to a depth of 5 cm from the inlet borehole surface. Two sub samples were impregnated in the laboratory with ^{14}C-MMA to investigate if the MMA resin intruded to a depth of 5 cm from the inlet borehole and was autopolymerized in the rock. The result was negative indicating that the MMA had evaporated from the test bore hole during one and half a years and had not polymerized in the porespace. However the fluorescence colourant stayed on the pore walls.

a)

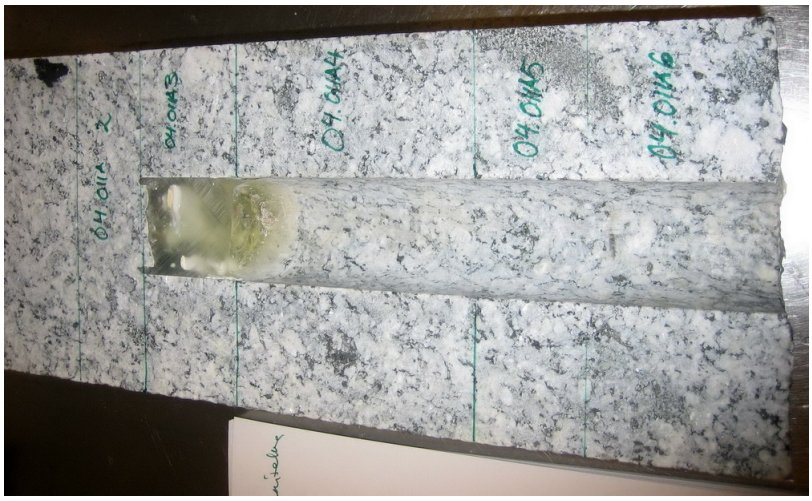

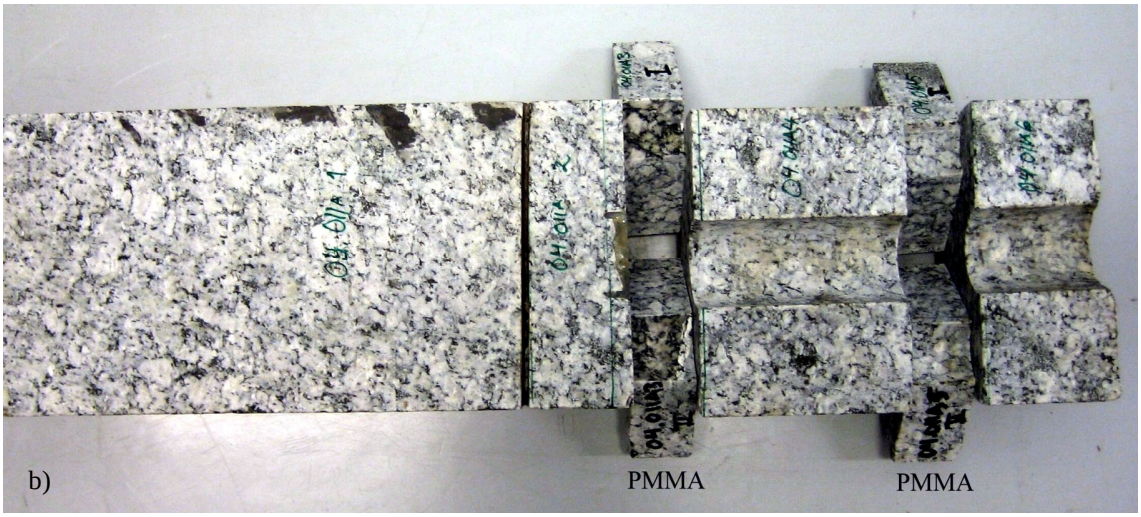

Fig. 13: a) Half of the overcore of PSG 04.011-OC that was sent to HYRL and b) a photo image showing the samples that were impregnated with ^{14}C-MMA in the laboratory

3.2 Heating test for polymerisation of MMA in situ

1.25 % of bentsoylperoxide (BPO) was added to the ^{14}C-MMA resin solution as an initiator to ensure the thermal polymerisation process. In order to polymerise the MMA *in situ*, the entire resin-impregnated rock mass had to be heated to 42° C to allow polymerisation to be initiated. The resin-impregnated rock mass was heated using a heater system in the central borehole in the same way as it was done in earlier experiments by Möri et al. (2003). It was important to know the heat input required in the central hole to allow polymerisation to take place at depth in the rock mass.

The heating tests with MMA were performed in the laboratory at the University of Helsinki using the block scale rock sample; Kuru grey granite block of (30 × 30 × 30) cm in size and *in situ* at the Grimsel Test Site using a borehole arrangement that provided various distances from the central hole where the rock temperature could be measured. Here it is emphasized that in the laboratory the starting temperature was about 22° C while at GTS the temperature was about 14° C.

3.2.1 Block scale heating tests in the laboratory

Fig. 14 shows the heating tests performed in the Kuru grey granite blocks. The *in situ* conditions were simulated in the block scale experiments by intruding ^{14}C-MMA into the water-saturated Kuru grey granite (permeability 10^{-18} m^2, porosity of 0.4 %). The heating equipment was placed in the central borehole after ^{14}C-MMA injection and temperature sensors were placed in the observation boreholes at distances of 2 cm, 4 cm, 6 cm and 7.5 cm. The heating oil was placed into the heater tube and between the surface of the injection borehole and the heater tube there was about 0.5 mm zone of ^{14}C-MMA. Heater temperature of 125° C was enough to produce temperatures above 40° C at all relevant distances and induce polymerisation, as seen in Fig. 15 which presents the results from one of the block scale heating tests. Total thermal polymerisation time was 72 hours and the impregnated MMA was fully polymerized in the rock pore volume. Thermo couples were placed in the observation boreholes without glycerol which could have improved the temperature measurement accuracy.

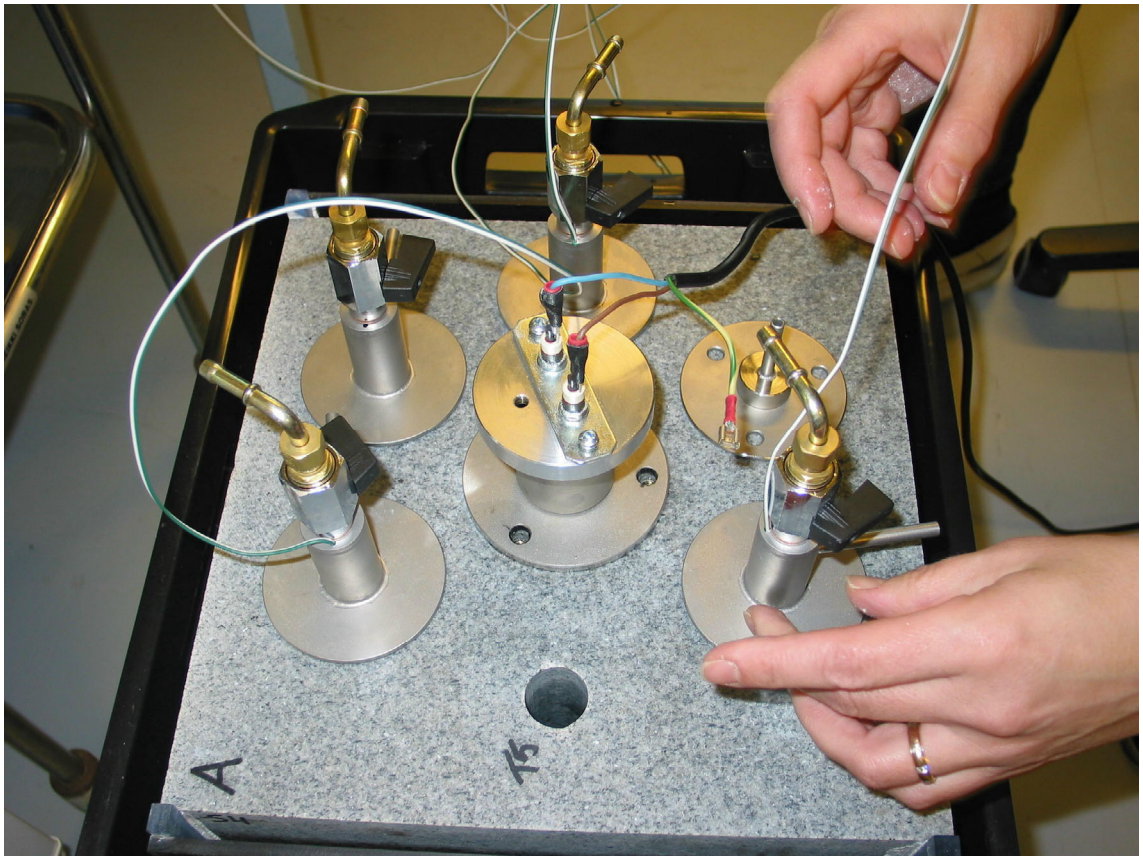

Fig. 14: Heating test for the Kuru grey granite block in the laboratory

HYRL/STUK heating equipment (including plugs, thermocouples and Data Acquisition Equipment)

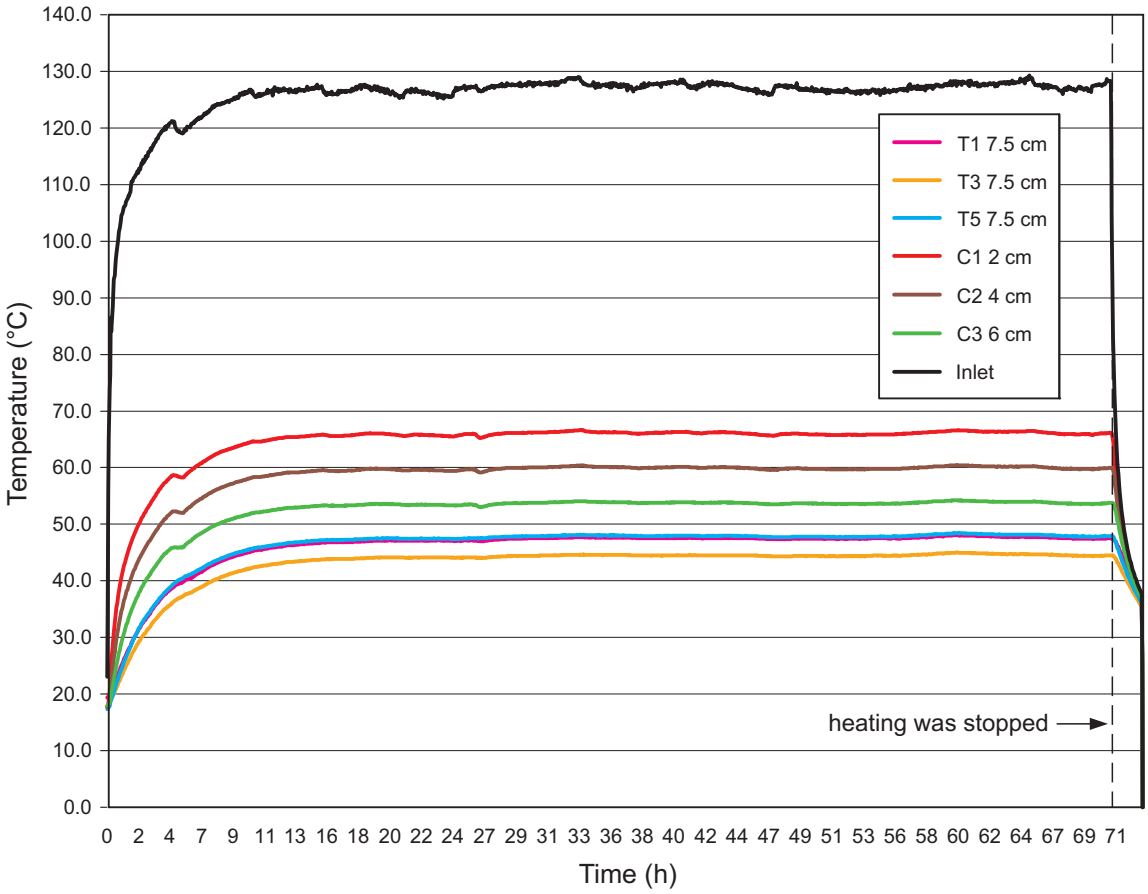

Fig. 15: Results from the block scale heating test

Distances from the heating borehole: 2 cm (C1), 4 cm (C2), 6 cm (C3) and 7.5 cm (T1, T3, T5)

3.2.2 *In situ* heating tests at GTS

Two heating tests were performed *in situ* at the Grimsel Test Site with HYRL/STUK heating equipment (including plugs, thermocouples and Data Acquisition Equipment), both lasting four days (26.-30.4.2004 and 3.-7.5.2004). The thermal polymerisation step requires a good heat distribution through the matrix to ensure polymerisation of the impregnated resin. The heater element was placed in borehole PSG 04.002 and temperatures were observed from the observation boreholes PSG 04.003, PSG 04.004 and PSG 04.005. Distances from the heating borehole were 7.5 cm, 15 cm and 30 cm respectively, as seen in Fig. 16. The temperature of the heating element was also followed. In these tests there was a 0.5 mm wide air zone between the heating element surface and the borehole surface which prevented maximum heat transfer from the heater to the rock.

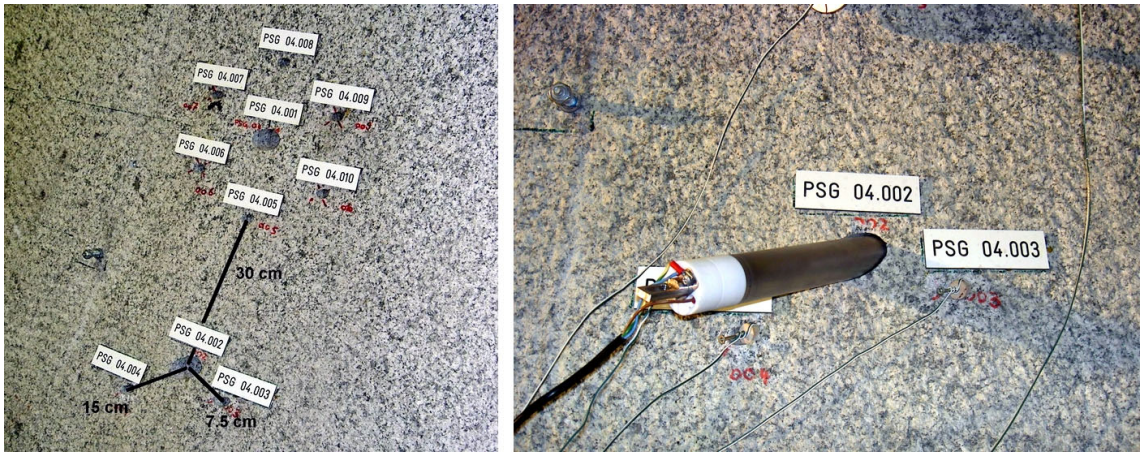

Fig. 16: Heating tests at GTS were performed from borehole PSG 04.002 to three boreholes at 7.5 cm, 15 cm and 30 cm distances from the heater using equipment from HYRL/STUK

The results from the heating tests are shown in Figs. 17 and 18. The maximum heater temperatures in the tests were 130° C and 150° C and measured temperatures from the observation boreholes were 30° C for the two nearest boreholes and 20° C for the borehole at a distance of 30 cm. In these tests the measured temperature values were lower than expected; the required 42° C was not reached. In the real case we did not have an air gap (0.5 mm) between the heater and the rock surface but the space was filled by MMA which should have improve the heat transfer from the heater to the rock. It would have been possible to add glycerol into the observation boreholes (Möri et al. 2003) to make sure of proper temperature measurement. From the test results it was decided to heat to more than 150 °C to ensure the required 42 °C at a distance of 15 cm from the injection borehole.

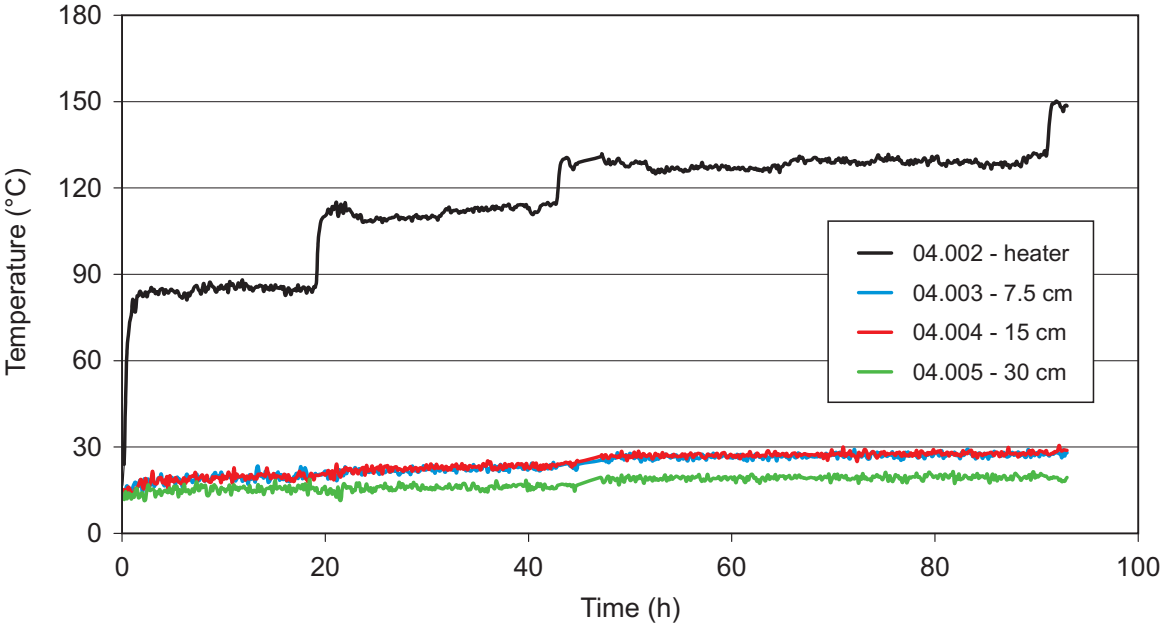

Fig. 17: Result from the first *in situ* heating test

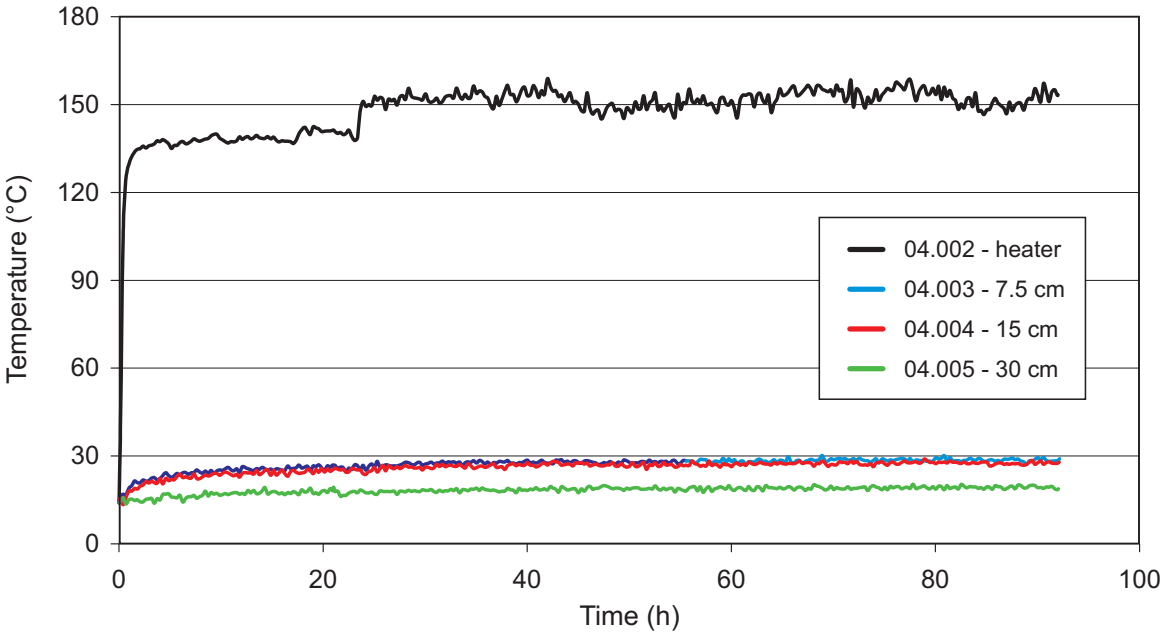

Fig. 18: Result from the second *in situ* heating test

4 ^{14}C-methylmethacrylate impregnation *in situ*

Although the level of radioactivity for the experiment was below the exemption limit and did not require a licence the experiment was discussed with the Swiss Federal Nuclear Safety Inspectorate (HSK) and permission was granted to use the radioactive resin *in situ* at the GTS. The *in situ* experiment consisted of four main field activities:

- Drying of rock matrix
- *In situ* injection of ^{14}C-MMA resin
- Heating of rock matrix around injection hole to polymerise ^{14}C-MMA in the matrix open pore volume
- Large diameter overcoring of the resin-impregnated rock matrix

In the following sections the first PMMA *in situ* impregnation is presented.

4.1 Drying of rock matrix

One of the disadvantages of the PMMA technique compared to other resin used for *in situ* rock impregnation is that the MMA monomer can not displace water from the pore space within the rock. Water-saturated conditions will inhibit the injection and it is therefore necessary to dry the rock matrix prior to the injection.

After the initial site selection was completed, the WT tunnel at the GTS was closed off and the tunnel ventilation increased which initiated drying of the rock matrix. Previous studies at the GTS have suggested that the matrix is not fully saturated till around 1.6 metres from the tunnel surface (Vomvoris and Frieg, 1993). This is backed up by recent work performed in the AU gallery of the GTS based on ^{4}He measurements (Andreas Möri, personal communication) which suggests that our injection interval (1.00 – 1.20 cm) might be in the partially desaturated zone.

A system designed at the University of Helsinki allowed drying of the rock matrix via down hole circulation of dry air. The system is shown in Fig. 19. A small pump drives the circulation and the air is dried by passing it through a dessicator containing silica gel (about 500 g). The silica gel had to be dried in an oven on a daily basis. The air ventilation of the injection borehole and the six outer boreholes lasted 17 days, started on 23.4.2004 and was stopped on 10.5.2004.

The capacity of the amount of air that was circulated in the tubes was not sufficient to dry the rock matrix properly, especially when the circulating air was not heated.

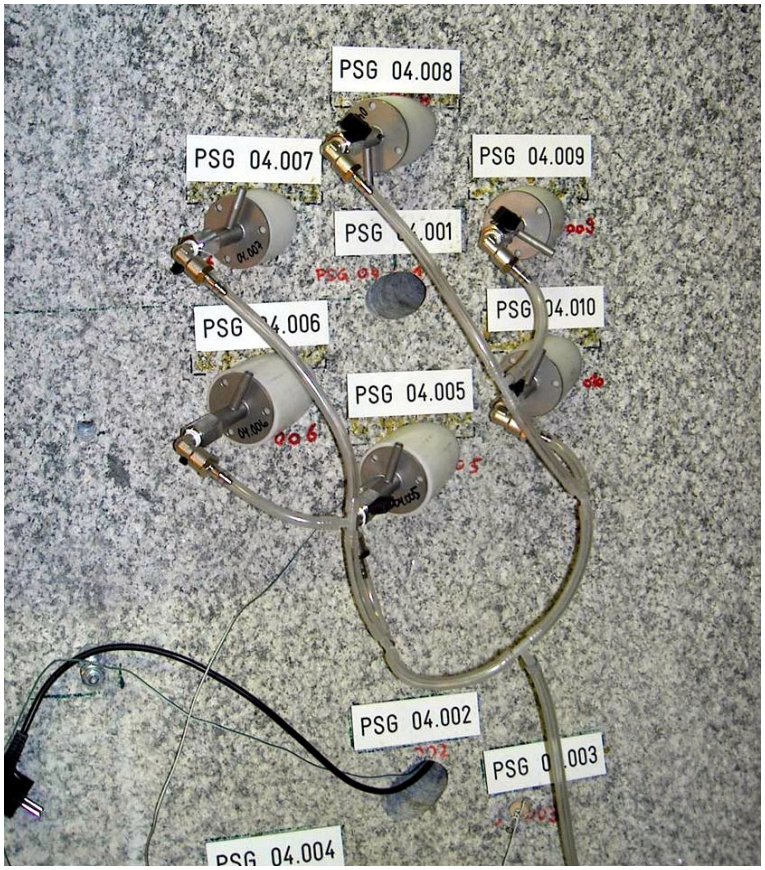

Fig. 19: Air ventilation system for drying the rock matrix. Picture was taken before the ventilation tube was installed into the injection borehole

4.2 In situ injection of ^{14}C-MMA resin

During planning of the PSG project, particular attention was paid to the packer system which would be used to inject the resin into the pore space of the rock. In the earlier Nagra/JNC (now JAEA) Connected Porosity experiment, an acrylic resin, NHC-9, was injected into a packed off interval. Once resin injection was completed, the packer system was removed and the borehole was filled with heating oil and a heating element was inserted. The purpose of the heating oil was to enhance heat conduction between the heating element and the borehole wall (Möri et al. 2003).

Although some of the basic system design could be carried forward to this experiment, the use of radioactive resins in this experiment made the removal of the resin packer undesirable due to the potential for contamination of the test site. Therefore a heating unit was integrated into the resin injection packer. This allowed the resin injection to be stopped and the polymerisation stage to begin without any removal of equipment. The MMA filled the open space between the packer and heating system and the borehole surface. A schematic diagram of the packer system is shown in Fig. 20.

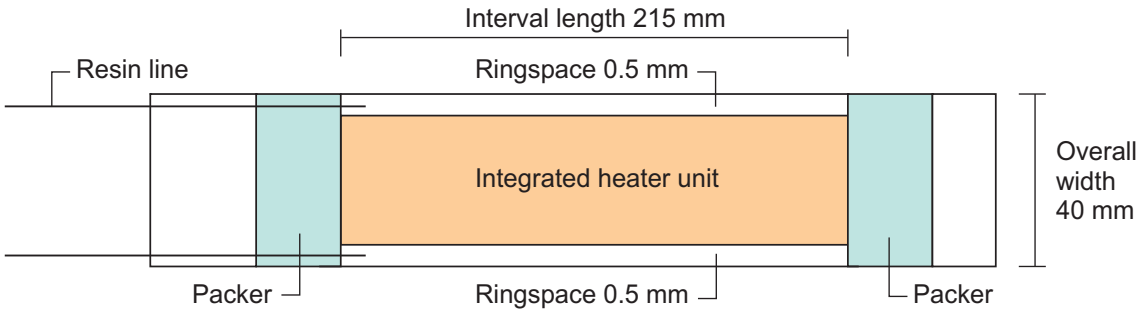

Fig. 20: Schematic diagram of the integrated resin injection packer and heater used for the *in situ* injection in the PSG experiment

The distance between heater and the borehole wall was 0.5 mm; this allowed the best heat conduction possible. The heater also acted as a dummy to minimise the volume of resin required. The location of the various intervals once the packer was inserted is given in Tab. 4.

Tab. 4: Downhole positioning of the PSG injection packer

Depth along borehole (mm)	**Length of interval** (mm)	**Instrumentation**
0 – 82	82	Borehole open
82 – 89	7	Packer
89 – 110.5	21.5	Test interval
110.5 – 117.5	7	Packer
117.5 – 127	9.5	Dead volume, open (ringspace)

^{14}C-MMA injection details

In total 8.0E+06 Bq of ^{14}C doped MMA was transported from the University of Helsinki to the GTS. This was diluted into 400 mL of inactive MMA. Thus the ^{14}C-MMA activity that was used for the *in situ* impregnation experiment was about 20 kBq/ml. 5 g of BPO (bentsoyl peroxide) and 0.1 g fluorescent dye (EpoDye) were added and the solution was thoroughly mixed. It was important to keep the MMA solution in cool and dark conditions to prevent any spontaneous polymerisation of the resin.

The resin injection system was manufactured and installed at the GTS by Solexperts AG. The layout of the *in situ* experiment is shown below in Fig. 21. A small resin injection vessel was placed on a high-precision balance and PEEK (polyether-ether-ketone) lines were used to connect the injection vessel to the injection packer, which was placed in the central borehole. The balance was connected to a data acquisition system which allowed the mass of resin injected and the resin injection pressure to be continually recorded. The system was pressurised by nitrogen gas. The air-flushing from the observation boreholes was stopped when the impregnation started.

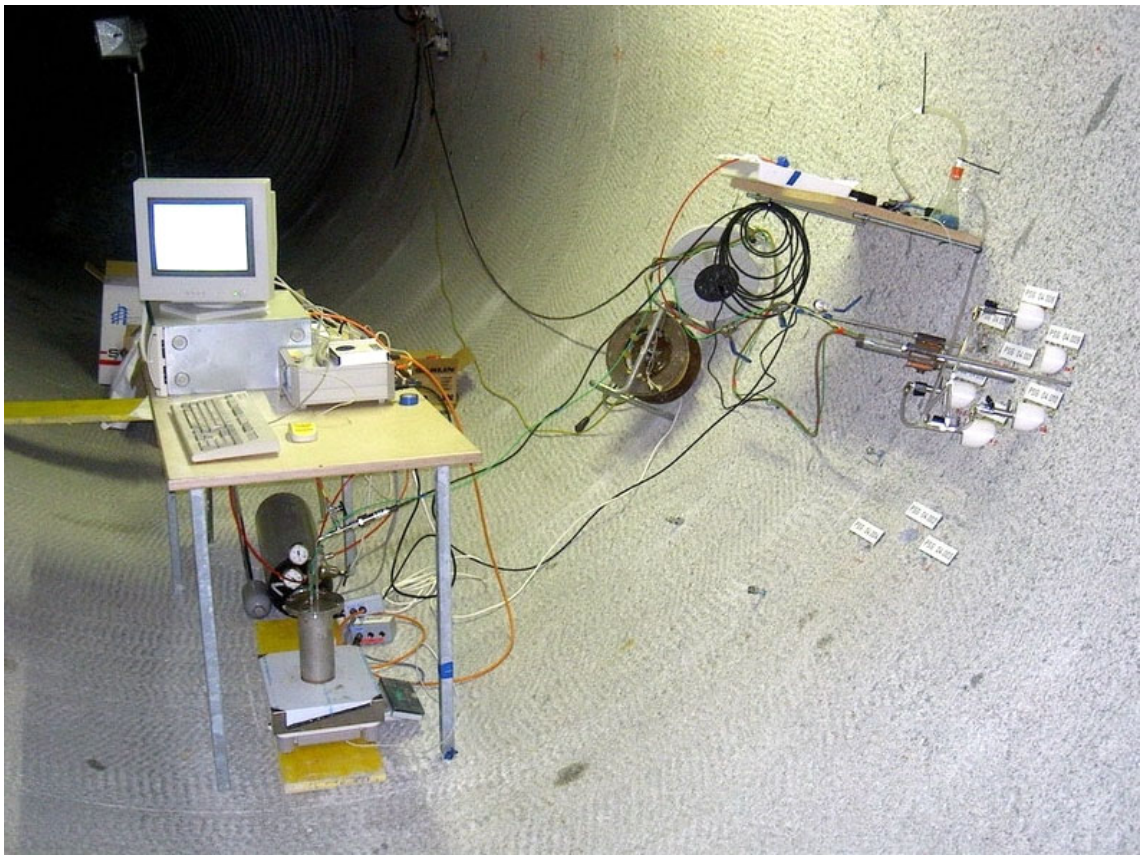

Fig. 21: The *in situ* resin injection equipment at the GTS. The injection vessel can be seen under the desk. The installed packer system is on the right hand side

Resin injection began on 10th May 2004 and injection continued until 14th June 2004. In total 50 mL of ^{14}C-MMA had intruded into the rock matrix in four weeks. Initially the injection of resin was fast but this gradually slowed down through the course of the experiment. Vacuum pumping from the observation borehole PSG 04.005 below the injection borehole did not cause a significant increase in the flow rate. As the permeability of the granodiorite matrix was known to be about 10^{-18} m^2 it was postulated that the vacuum should affect the intrusion rate of MMA. The injection pressure was increased stepwise manually (see red line in Fig. 22).

Initial tests in the laboratory indicated that the autopolymerisation of MMA was not likely. However the MMA resin was totally polymerized when the system was opened at the end of injection on 14th June 2004. A peak in the pressure curve was found on 2nd June 2004 which was thought to indicate the autopolymerisation of ^{14}C-MMA in the resin injection vessel. It was not known at the time if the ^{14}C-MMA had polymerized in the rock matrix and the work was continued as originally planned.

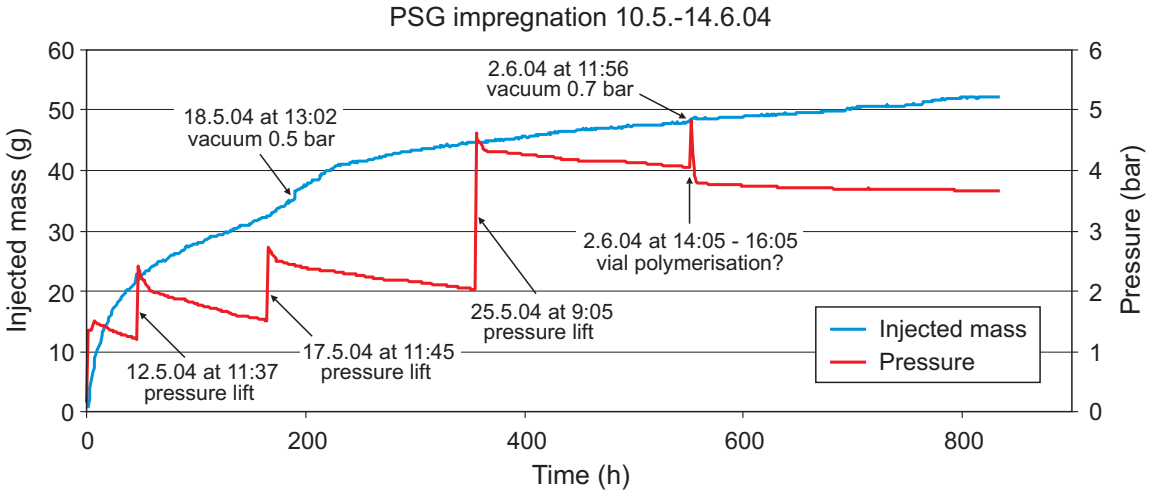

Fig. 22: Monitoring data for the PSG experiment. The injected mass of resin and the injection pressure are plotted as a function of time

4.3 Polymerisation

After the resin injection was stopped, the injection vessel was opened and it was discovered that the resin had spontaneously polymerised. Not only was the resin that had not been injected polymerised but also the resin in the injection tubing was solid. The reason for the auto-polymerisation is unknown. It was suspected that the contact of the resin with the metal equipment might have initiated the polymerisation, but this is not in agreement with earlier pot life experiments. In the laboratory the ^{14}C-MMA resin was placed both in an aluminium chamber for 2.5 months in a vacuum as well as in stainless steel pressure vial for 1.5 months under 5 bar pressure in nitrogen atmosphere. In both cases MMA remained in liquid form.

Heating of the rock mass took place to ensure that the resin in the pore space had also polymerised. This lasted 16 days, starting on the 14th June 2004 and finishing on the 30th June 2004. Two heating units were used. In the injection borehole (PSG 04.001) was the Solexperts' integrated injection/heating system which had MMA filled space between the heater and the borehole surface. The HYRL/STUK heater element which had air between the heating element and the borehole surface was in borehole PSG 04.002. The temperature sensors were installed in boreholes PSG 04.005 and 04.006. Furthermore two small glass vials filled with inactive MMA and BPO were placed in boreholes PSG 04.008 and PSG 04.010 (see Fig. 23).

Paraffin oil was added into the observation boreholes, however the temperature sensors did not reach the oil as planned as planned. Fig. 24 shows the results of the temperature measurement during thermal polymerisation. The temperature in the injection borehole heating element reached 180° C. Temperatures that were measured from observation boreholes PSG 04.005 and PSG 04.006 at a distance of 15 cm from the injection borehole were about 30° C. According to this result the required 40° C was not reached at this depth. However the measured temperatures might have been lower than expected due to the fact that the sensors were not in the paraffin oil. In the block scale tests the required 40° C at a depth of 7.5 cm from the inlet hole was obtained by heating the inlet hole to 125° C in the inlet hole. In addition the inactive MMA vials in the observation boreholes were both polymerised within four days after the heating was started which indicate that the temperature was high enough but the measurement was poor.

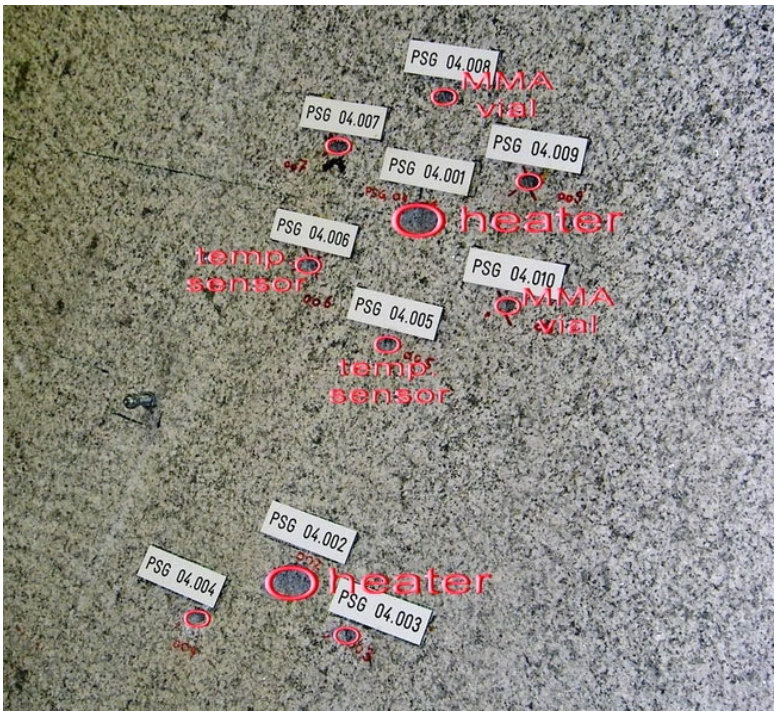

Fig. 23: Distribution of heaters and sensors in the PSG boreholes

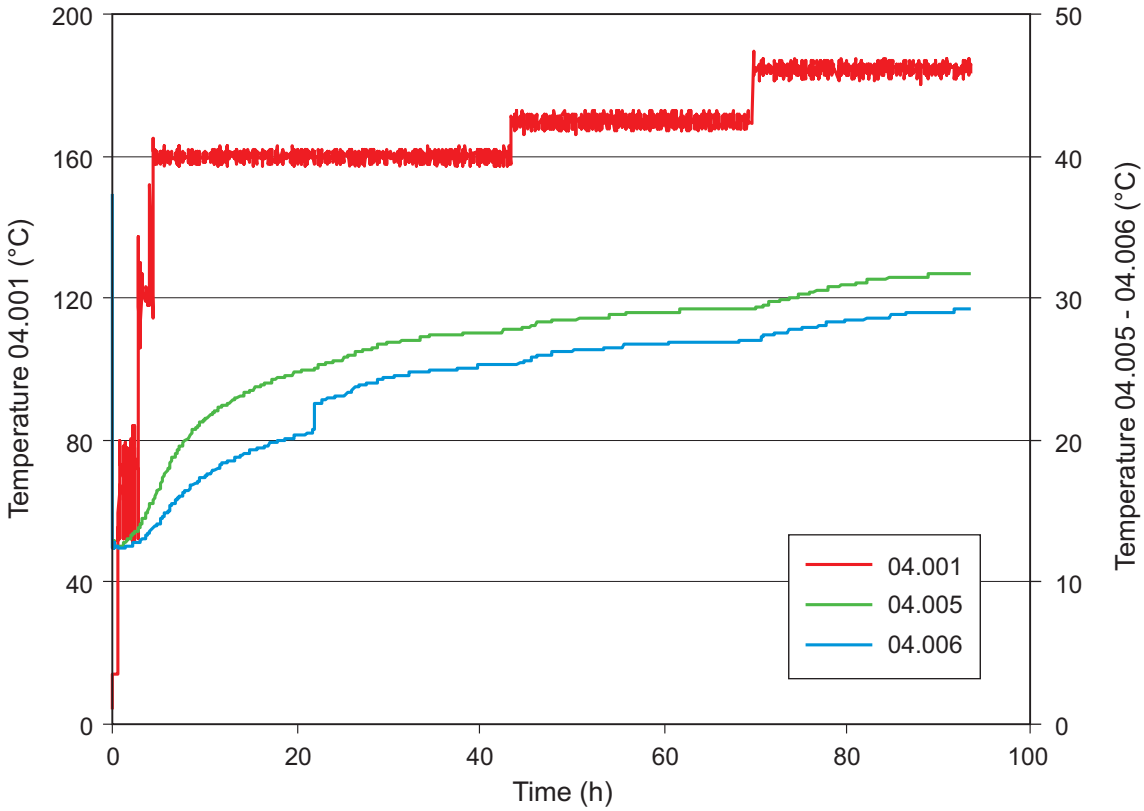

Fig. 24: Heating graph for the PSG experiment during the polymerisation stage
(red line: temperature of heating element)

4.4 Overcoring

Overcoring was performed with a Hilti drilling machine using a single core barrel (outer diameter = 300 mm, length = 80 cm). The maximum length of core that could be removed in one piece was limited by the length of core barrel. The diameter of the overcore was 290 mm. The overcoring equipment is shown in Fig. 25.

Fig. 25: Overcoring of the PSG experiment by Hans Aplanalp

Overcoring was performed in two drilling sections: 0 – 0.55 m and 0.55 – 1.17 m. The overcore finished at the lower end of the second packer. The observation borehole contained small amounts of resin. This resin was still gel-like indicating incomplete polymerisation at a depth of 15 cm from the injection borehole.

Prior to starting overcoring it was planned to remove the packer system containing the injection devices as well as the heater. However the system could not be removed as the packer tube was broken when the field crew tried to pull out the system. The reason for this incident is twofold: 1) The resin had polymerised already during the injection phase and had therefore a very good connection with the borehole walls in the test interval, (moreover additional heating did not help). 2) The packer system was not designed to sustain high pulling forces as would be required to remove it in this case.

However, it was shown that the packer system would neither hinder nor negatively influence the overcoring / core extraction procedure. The system remained closed preventing loss of resin and

decreasing artefacts caused by drilling. This would allow a detailed investigation of the borehole disturbed zone (BDZ) around the central injection borehole.

Both core sections showed good core quality and no core losses were observed. A first evaluation of the core surfaces with the UV lamp showed no traces of the fluorescein doped resin. On the other hand resin was found in the lower packer position. The core surfaces at the top and at the bottom of this core section had no resin. The structural homogeneity of the matrix that was already observed in the drill cores and the borehole walls of the central borehole was not confirmed by the overcoring. However inspection by naked eye confirmed that in centimetre scale the rock texture is homogeneous but foliated; with no open flow paths found in any of the rock sample studied.

4.5 Radiation Protection

No accidents or incidents took place during the PSG experiment and at no time were any dose rates measurable. The over core produced could be classified as non-radioactive as the concentration of ^{14}C activity was below the exemption limit. No radioactivity was released to the environment during this experiment and no ^{14}C remained *in situ*. The addition of the fluorescent tracer to the resin provided an easy way to monitor for any spillages of the ^{14}C doped resin as the fluorescence was much easier to detect than the very weak beta emissions of the ^{14}C tracer.

4.6 Sub-Sampling

The overcore 04.001-OC which was 80 cm in length and 30 cm in diameter was sent to University of Helsinki in Finland. The core was sawn in the Technical Research Centre of Finland (VTT) using a large diamond into 5 slices of about 5 cm in thickness each as shown as seen in Figs. 26 and 27. It is emphasized that when making the sub-samples mechanical artefacts cannot be avoided when using big diamond saws. These artefacts increase the sub samples total porosities due to grain boundary pore openings which get wider and a few intra- and inter granular micro fissures might be formed to depths of 1-2 mm from the sawn surface.

Furthermore smaller sub-samples were cut from the slices for several porosity analyses methods using Masonry Coup diamond saw (blade diameter 25 cm) and Low Speed diamond saw (Buehler). The partitioning diagrams of the over core can be seen in Figs. 28, 29 and 30. Furthermore the sub-sample 04.001-OC-D-reimprenated was sawn into several smaller samples; partition diagrams shown in Fig. 30. Mercury porosimetry and water saturation gravimetry was performed on these sub-samples.

Fig. 26: Sub-sampling of the PSG over core 04.001-OC at VTT for further analysis

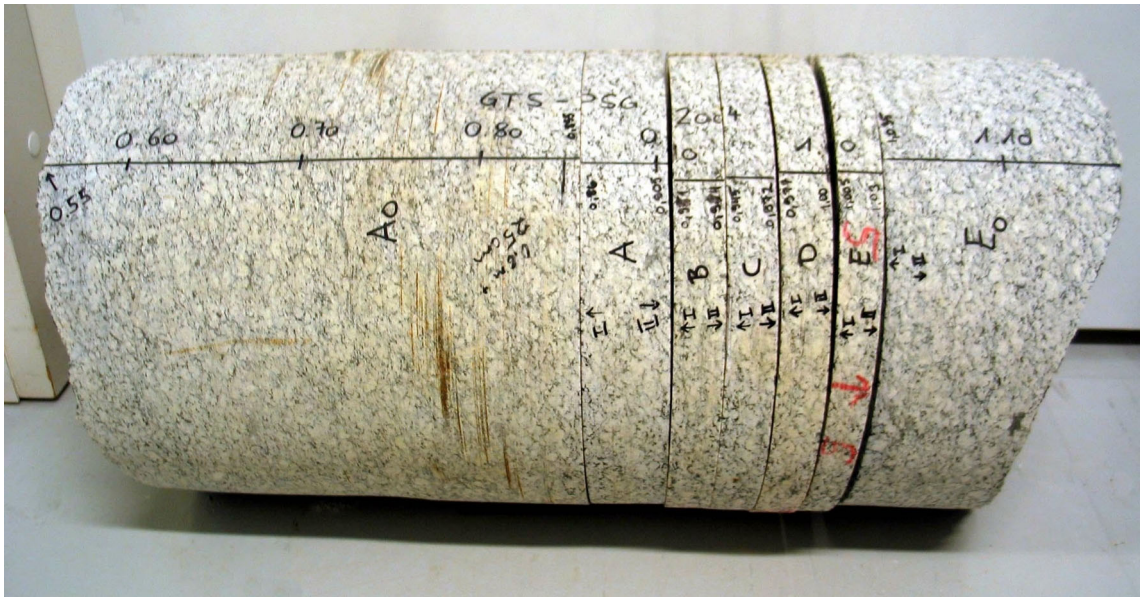

Fig. 27: The PSG over core 04.001-OC after sub-sampling

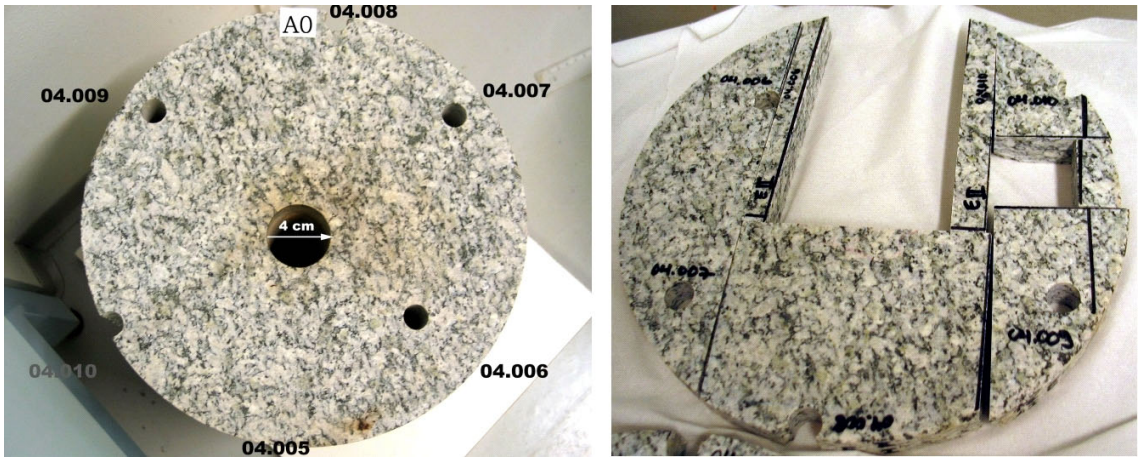

Fig. 28: Cutting the PSG over core 04.001 for sub-samples

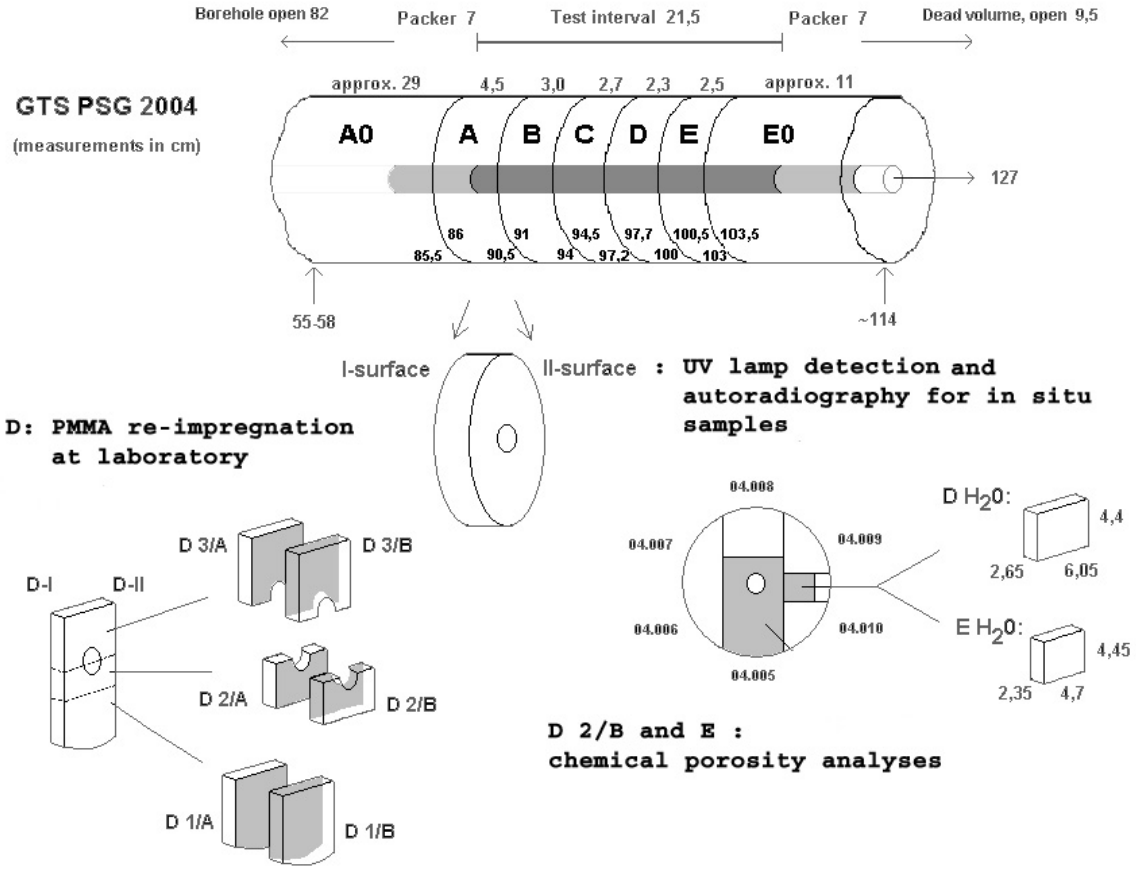

Fig. 29: Partition diagrams of the PSG 04.001-OC and sub-samples. Performed porosity analyses are presented

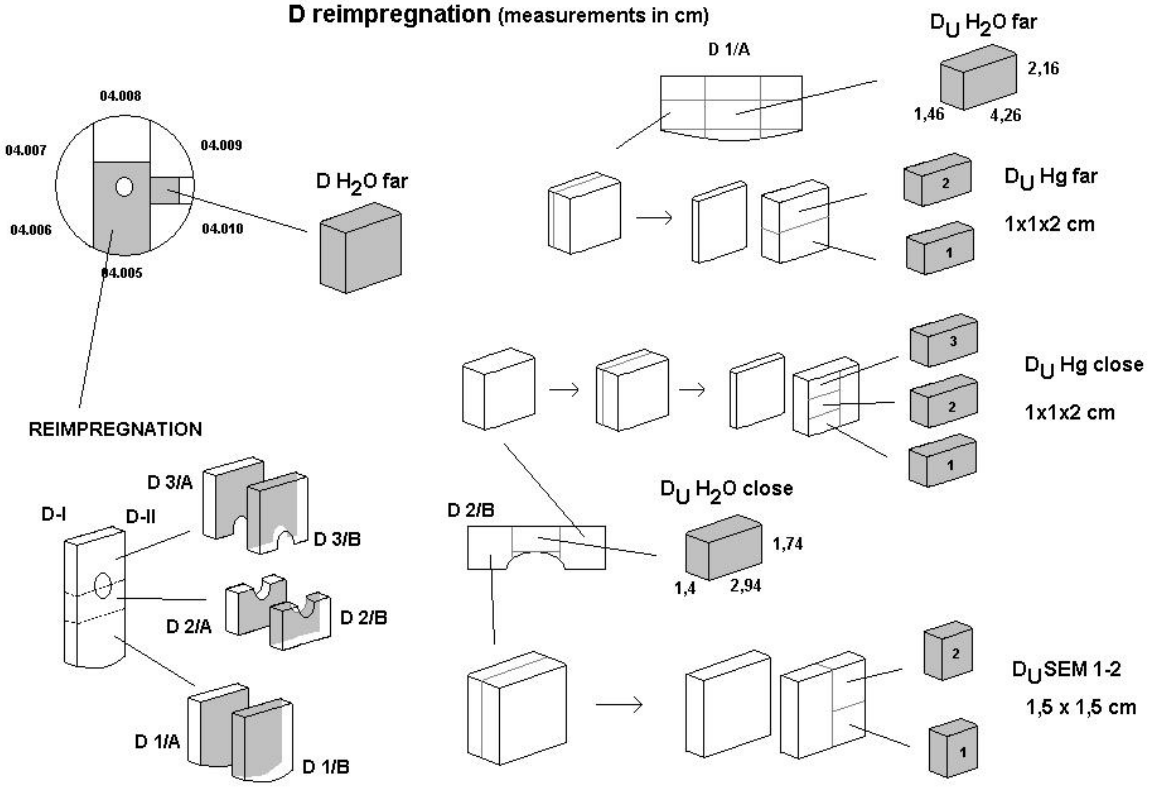

Fig. 30: Partition diagrams of sub-samples 04.001-OC-D-ri and the performed porosity analyses

4.7 Lessons learned

From the technical point of view *in situ* ^{14}C-MMA impregnation was successfully performed using the "know how" of earlier experiments done at GTS (Möri et al. 2003). The drying of the rock matrix might not have been sufficient but the weight loss of the MMA indicated that it intruded into the rock. Autopolymerisation of the acrylic resin was a drawback and the reason for that is not known. Overcoring could be performed as planned without any technical problems. The 80 cm long 300 mm single core barrel provided an intact drill core of 1.17 m length containing the test interval as well as the two packers. As the MMA polymerisation prevented the removal of the packers, for future *in situ* impregnation experiments the down borehole equipment should be designed so that it can be removed in one piece or the central tube as well as the injection lines should be independently removable after polymerisation has taken place.

5 Porosity results

Several porosity analysis methods were used for different *in situ* impregnated sub-samples sawn from the overcore 04.001-OC (04.001-OC-E and 04.001-OC-D). ^{14}C-MMA porosity was measured also for the core drilled from the injection borehole (04.001-IHC), and this was used to measure porosity in the laboratory. The aim here is to compare the lab and *in situ* porosities and to find the residual porosity, which is mainly the mechanical artefacts caused by sawing the sub–samples. In the following sections the comparisons are made between overcored *in situ* MMA impregnated sample and the laboratory MMA impregnated sample. After several autoradiography tests it was found that the ^{14}C-MMA activity was not enough to obtain ^{14}C-MMA autoradiographs for *in situ* porosity determination and one sub-sample (04.001-OC-D) was re-impregnated using normal ^{14}C-MMA procedure in the laboratory. In this experiment the residual porosity would have been filled by ^{14}C-MMA. With tracer activity high enough, the autoradiographs were sufficient for proper quantitative autoradiography porosity analyses. Sub-samples were analysed with water saturation, mercury porosimetry and chemical porosimetry based on thermogravimetry methods.

5.1 UV light examination of the PSG 04.001-OC slices

All sawn surfaces; A0, AI&II, BI&II…E0 (see Fig. 29), were exposed on autoradiographic film (Kodak Biomax MR) for 30 days. ^{14}C radioactivity was too low for accurate detection of MMA intrusion and hence quantitative porosity determination with the ^{14}C technique was not directly possible. However the intrusion depth could be measured roughly from the films. The radioactivity level was even too low for the digital autoradiography (FLA scanner) which was tested using two weeks exposure times. In addition the depths of resin intrusion could be measured with fluorescent imaging, which means that the UV-light detection was performed for all sawn rock slab surfaces. Tab. 5 presents the results of UV-light inspection. EpoDye doped methylmethacrylate was found at depths from 2 to 5 cm from the injection bore hole wall.

Tab. 5: Rock slabs of PSG core for analyses. MMA intrusion depths from film autoradiography and fluorescent imaging

slabs	**surface of slab**	**distance from tunnel wall** (cm)	**width of slab** (cm)		**autoradiography**	**fluorescence imaging**
A0		**85.5**			MMA intrusion depth (cm)	MMA intrusion depth(cm)
A	I	**86**	min	**3.81**	3	2
	II	**90.5**	max	**4.19**	3	2-3
B	I	**91**	min	**2.12**	4	4-5
	II	**94**	max	**2.2**	4	2
C	I	**94.5**	min	**1.84**	3	2
	II	**97.2**	max	**2.12**	4	2
D	I	**97.7**	min	**1.99**	4	4
	II	**100**	max	**2.25**	5	4
E	I	**100.5**	min	**1.44**	5	4
	II	**103**	max	**1.84**	5	4-5
E0		**103.5**			6	5

5.2. PMMA porosity results

5.2.1 Laboratory PMMA porosity results

First the porosity of 04.001-IHC was analysed in the laboratory by the ^{14}C-MMA method. Three samples coded as 04.001 IHC67-71 cm, 04.001 IHC71-75 cm, 04.001 IHC75-85 cm were impregnated. One sample was impregnated with high ^{14}C activity. Two samples were impregnated with low activity methylmethacrylate for tests with a new FujiFilm FLA 5100 scanner. The comparison between film autoradiography and digital autoradiography is presented in Kämäräinen et al. 2006. The main advantage of the digital autoradiography is that it is 50 to 100 times more sensitive and the linearity in the quantitative measurement covers four to five orders of magnitude compared to two orders of magniture maximum linearity in film autoradiography. The activities applied here were 888 kBq/ml and 37 kBq/ml. The MMA solutions of low activity were doped with fluorescent dyes, Epodye and Bluedye. The impregnation conditions for the three samples are shown in Tab. 6.

Tab. 6: Impregnation conditions for three IHC samples

	drying (d)	**max. temp.**	**impregnation** (d)	**tracer** (kBq/ml)	**dye**	**polymerisation**	**total dose** (kGy)
04.001 IHC 67-71	7	100 °C	14	37	Epodye	irradiation	71
04.001 IHC 71-75	7	100 °C	14	37	Bluedye	irradiation	71
04.001 IHC 75-85	6	100 °C	20	925	-	irradiation	65

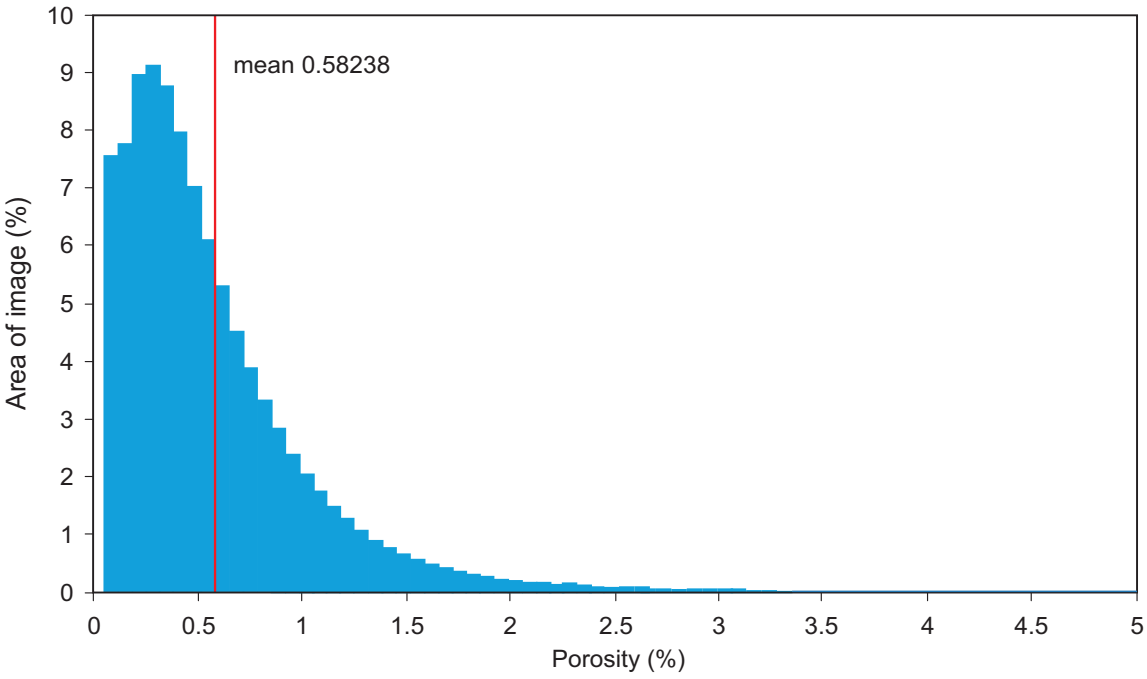

Fig. 31: Porosity histogram of sample 04.001 IHC 75-85 taken from the Mankeli (Matlab) porosity calculation program

Fig. 31 shows one example of the measured PMMA porosity histograms of sample 04.001-IHC 75-85. Fig. 32 shows the photo image of ^{14}C-MMA impregnated rock sample's surface, the corresponding autoradiograph and the superposed image. Different shades of gray on the autoradiograph, represent different porosities; the darker the shade the higher the porosity. The superposed image shows the porosities over 1 % on the photo image of the rock surface. The porosity pattern is even and intra granular porosity was dominant. Biotite grains surrounding quartz and feldspar grains showed highest porosities; values over 2 % were detected. Intra granular porosity was also found in quartz grains; values of 0.5 % were detected. The total PMMA porosity of the sample was 0.6 %.

a)

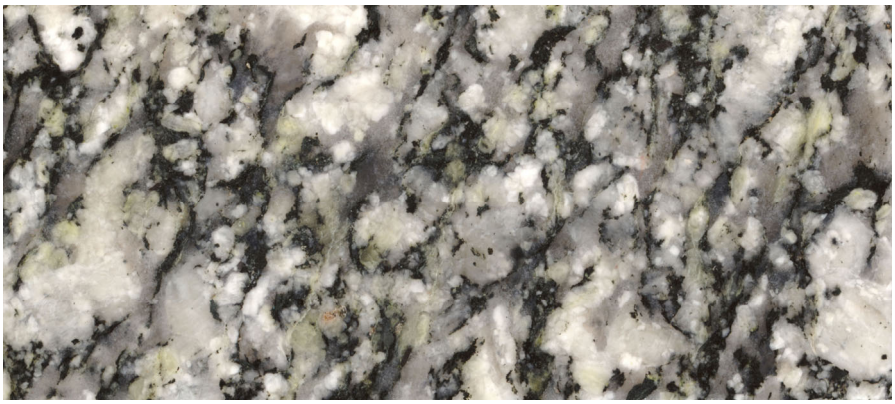

b)

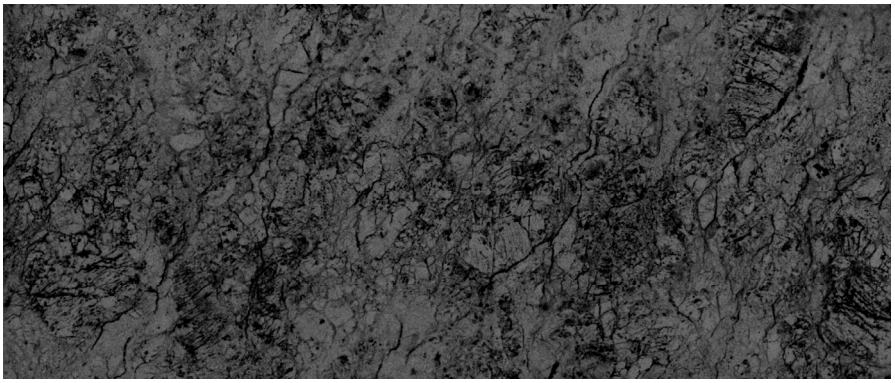

c)

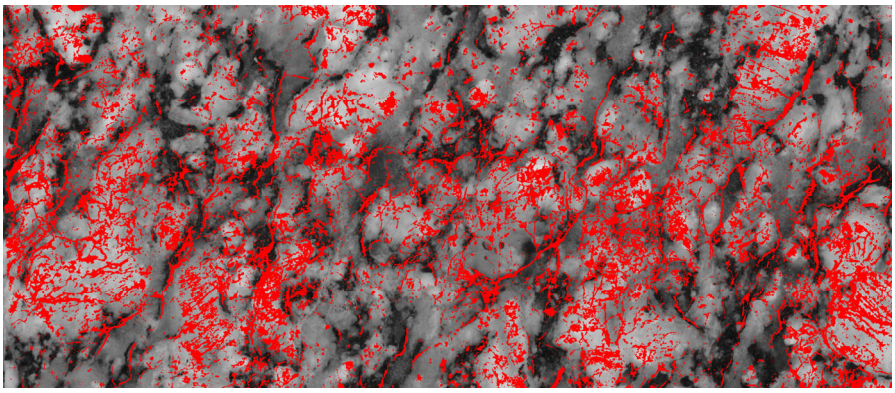

Fig. 32: Photo image of impregnated 04.001-IHC rock surface

a) rock sample surface b) corresponding autoradiograph and c) overlay of the auto-radiograph on the rock surface where red phases illustrates over 1 % porosities. Sample width is 5 cm. Total PMMA porosity detected was 0.6 %.

The connective pore space of different sized core samples of Grimsel Granodiorite were completely impregnated under laboratory conditions as found in this work and earlier experiments (Kelokaski et al. 2006) once the sample was properly dried. All minerals were found to be porous and could be visualized with PMMA autoradiographs.

5.2.2 *In situ* PMMA porosity results

The ^{14}C-MMA activity was 20 kBq/ml in the *in situ* experiment. 30 days exposure time on Kodak Biomax X-ray films was not sufficient to get dark enough images for pore space visualization by film autoradiography. Because the activity was too low to produce autoradiographs for quantitative porosity calculation, it was decided to re-impregnate one sub-sample in the laboratory to find out the amount of *in situ* intruded methylmethacrylate from the variation on the film darkness. The ^{14}C-MMA activity of 520 kBq/ml was used leading to exposure times of 10 days to get the autoradiographs that were good enough for quantitative porosity analyses.

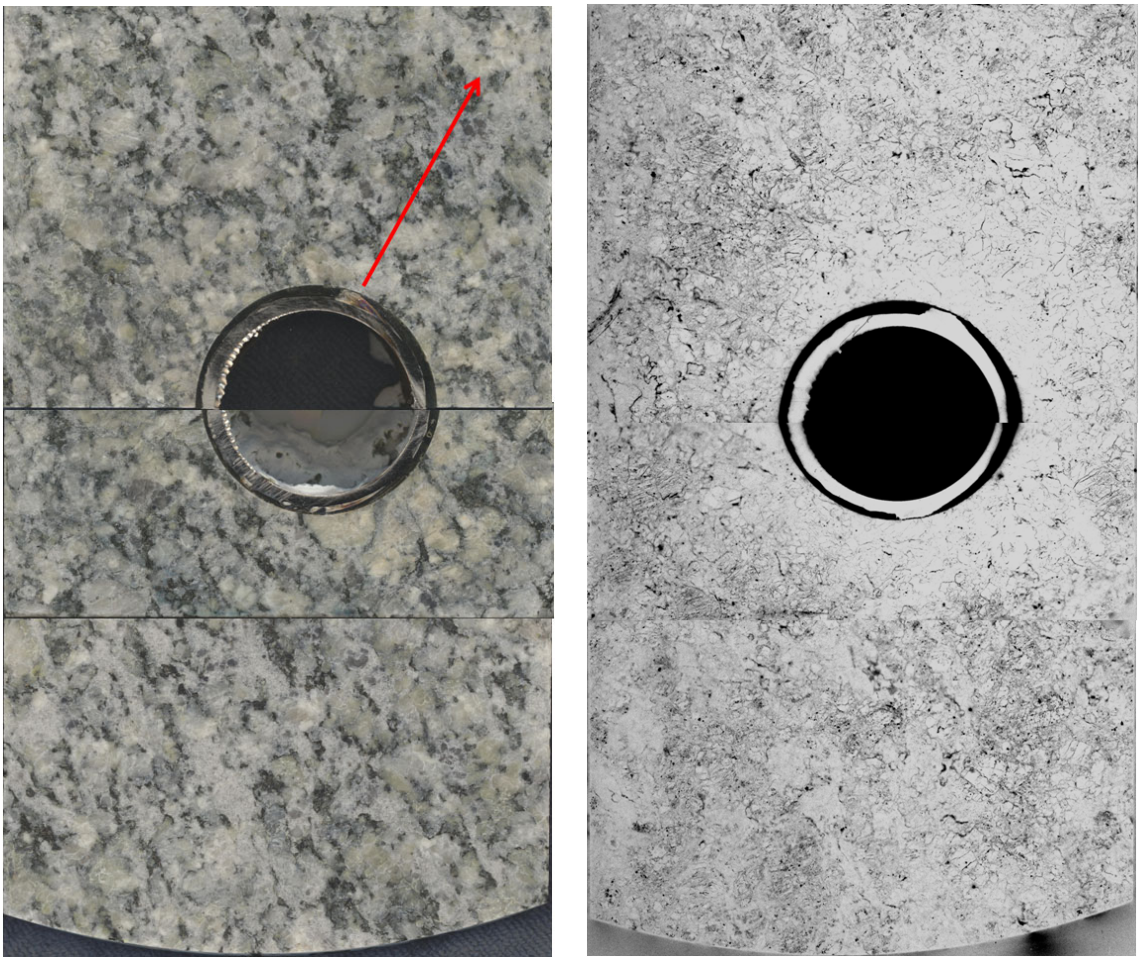

Fig. 33: a) Photo images of the reimpregnated rock slices 04.001-OC-D-ri (1A, 2A and 3A) b) and corresponding autoradiographs.

The profile (see Fig. 34) showing the residual porosity is measured according to the red arrow. Porosity values clearly increased from the injection borehole surface to depths of 2 - 5 cm indicating *in situ* MMA intrusion to these depths.

Fig. 33 presents the photo images of the re-impregnated rock slices (PSG 04.001-OC-D-ri, surfaces 1A, 2A and 3A) and the corresponding autoradiographs. The porosity profile was measured following a line on a photo image. What is seen on the autoradiograph now is the laboratory impregnated ^{14}C-MMA's activity. The exposure time was only 10 days compared to the 30 days exposure time that was used for *in situ* impregnated sub-samples thus the darkening on the film is caused only from the laboratory impregnated methylmethacrylate. This activity corresponds to the residual porosity after the *in situ* impregnation (see Fig. 34). The mechanical artifacts, stress release and PMMA contraction causes the residual porosity in the sub-sample. The residual porosity increased from 0.1 % to 0.55 % from the injection borehole to a depth of 5 cm. The FLA scanner image is shown in Appendix 1. In this method the exposure time was only 20 hours. Different shades of blue colour on the FLA scanner image represent to different porosities; dark blue presents about 0.1 to 0.2 % porosities whereas light blue presents about 0.5 to 0.6 % porosities.

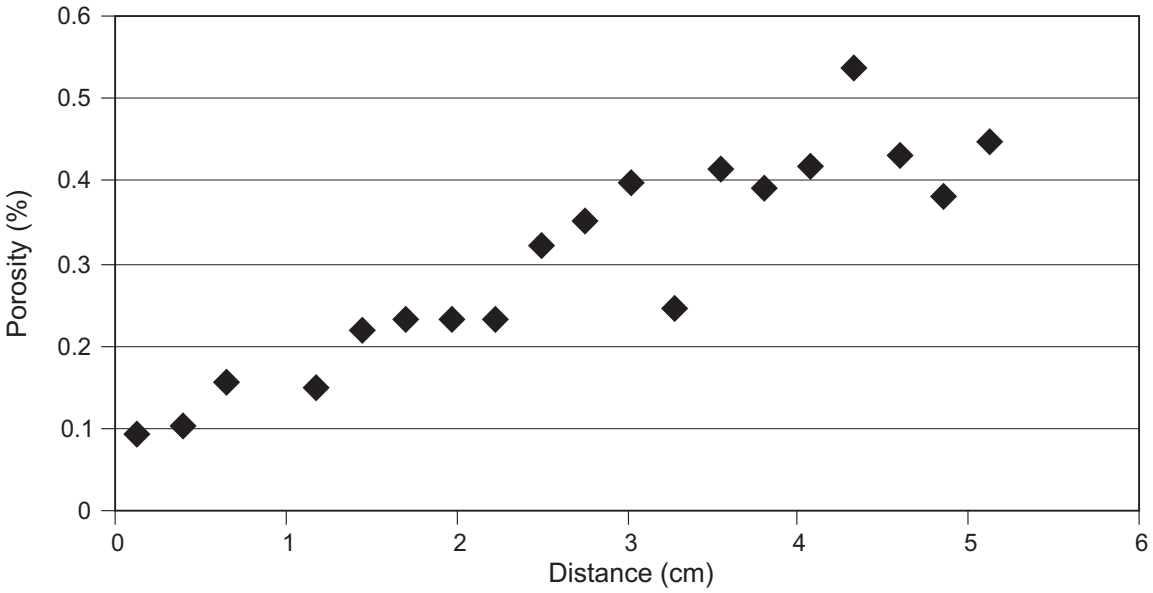

Fig. 34: Porosity profile showing the residual porosity in the sub-sample 04.001-OC-D–ri. Porosity values clearly increased from the injection borehole surface to a depth of 5 cm.

5.3 Water saturation gravimetry results

04.001-IHC

Five samples from the 04.001-IHC core were taken for water saturation gravimetry. Samples were 2 to 4 cm in length and 4 cm in diameter and coded IHC3-6 cm, IHC6-9 cm, IHC9-12 cm, IHC56-59 cm and IHC59-63 cm where the 3 – 6 cm etc. shows the depth from the tunnel wall surface. The results are shown in Tab. 7 and are graphically represented in Fig. 35.

Tab. 7: Results of water impregnation measurements on 04.001-IHC injection bore hole core material

	volume (cm^3)	**dry mass**	**sat. mass**	**density** (md)	**density** (sm)	**porosity** [1] (%)	**porosity** [2] (%)
IHC 3-6 cm	30.7907	83.3150	83.5101	2.7058	2.7122	0.48±0.03	0.53±0.03
IHC 6-9 cm	31.2184	84.0150	84.2113	2.6912	2.6975	0.47±0.03	0.57±0.03
IHC 9-12 cm	27.7972	76.0470	76.2221	2.7358	2.7421	0.48±0.03	0.54±0.03
Average close						**0.48**	**0.55**
IHC 56-59 cm	37.7629	102.8340	103.1659	2.7231	2.7319	0.69±0.04	0.78±0.04
IHC 59-63 cm	35.3095	95.4990	95.8058	2.7046	2.7133	0.68±0.04	0.77±0.04
Average far						**0.69**	**0.78**

[1] after 4 days saturation
[2] after 27 days saturation

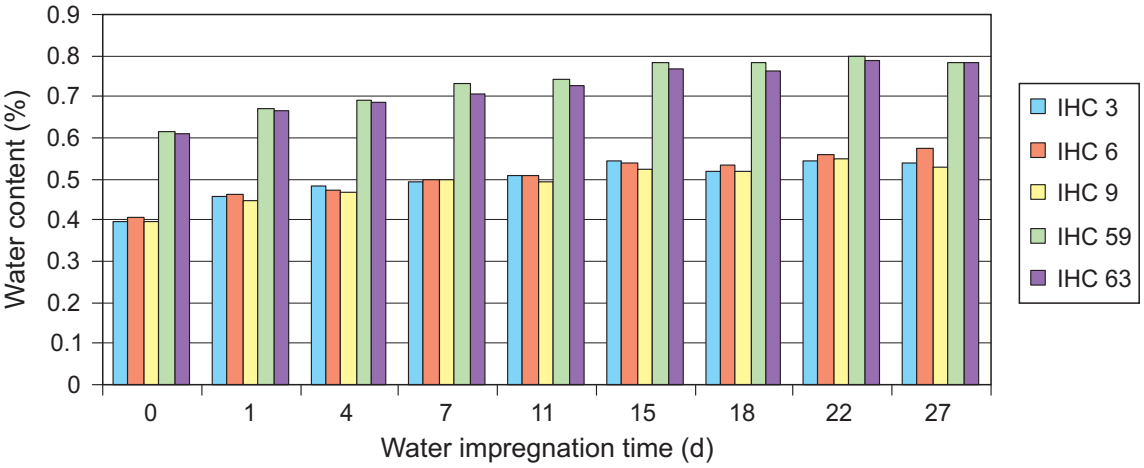

Fig. 35: Water saturation gravimetry results for 04.001-IHC.Variation in water content presented as a function of impregnation time

The water porosities were measured from samples located 3 – 12 cm and 59 – 63 cm from the tunnel wall, which is not as deep as the *in situ* injection interval at 89 – 110 cm from the tunnel wall. The porosity values after two weeks saturation time did not increase anymore indicating complete water intrusion into the rock matrix. Thus sample porosities varied between 0.48 % and 0.78 %; close to the tunnel wall the values were significantly lower than deeper in the rock indicating the natural heterogeneity in the rock massif.

04.001-OC

Two samples; E_{H2O} and D_{H2O}, were cut for water saturation gravimetry from over cored *in situ* slices; 04.001-OC-E and 04.001-D (see Fig. 29 in Section 4.6). Water impregnation was measured for 43 days. The results show that the intrusion of water continues slowly for several days. This is clearly seen in Fig. 36. However after about two weeks the porosity values did not increase significantly. The porosity values measured were 0.82 % and 0.85 % and were higher than the 04.001-IHC sample porosity values.

Tab. 8: Results of water saturation gravimety

	volume (cm^3)	**dry mass**	**sat. mass**	**density** (md)	**density** (ms)	**porosity** [1] (%)	**porosity** [2] (%)
D $_{H2O}$	70,5430	192,3300	192,9600	2,7264	2,7354	0.66	0.82
E $_{H2O}$	49,1503	132,7200	133,1900	2,7003	2,7099	0.67	0.85

[1] after 3 days saturation
[2] after 36 days saturation

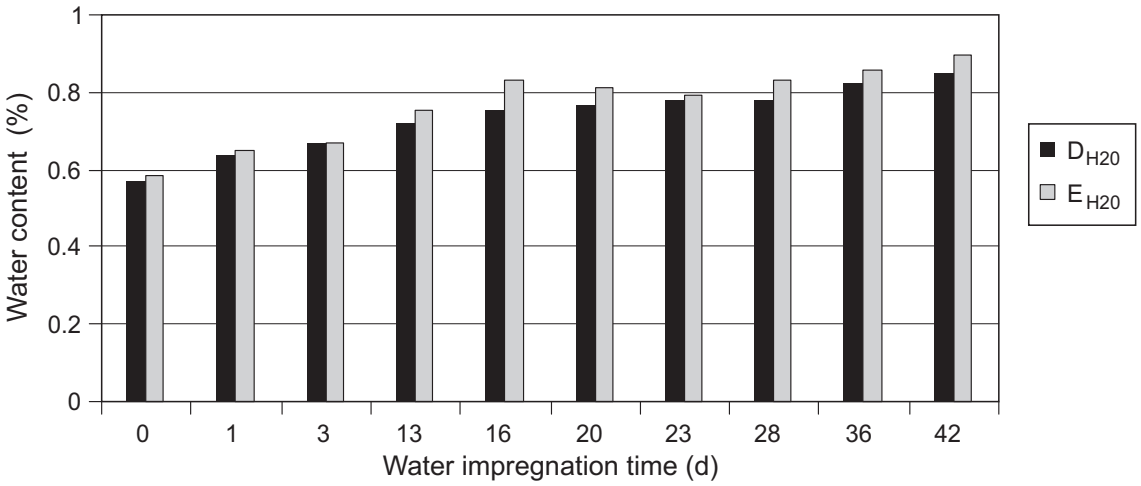

Fig. 36: Variation in porosity as a function of impregnation time for sub-samples 04.001-OC-E_{H2O} and –D_{H2O} (see Fig. 28).

The two sub-samples E_{H2O} and D_{H2O} were taken from a depth of 5 cm from the injection bore-hole surface thus representing non-impregnated matrix (see Fig. 29 in Section 4.6). However the samples were taken at a depth of 99 cm and 102 cm from the tunnel wall surface. The higher porosity values seemed to be reasonable if the porosity is increasing when going deeper into the rock from the tunnel wall. The difference between E_{H2O} and D_{H2O} sub-sample' porosities and 04.001-IHC sample porosities might also be the results of the stronger mechanical artefact for overcored sub-samples (04.001-OC-E and D) than for 40 mm diameter drill cores (04.001-IHC).

Two more sample porosities were analysed; $D_u$close (next to the injection hole surface) and $D_u$far (at a depth of 7 cm from the injection hole surface; see Fig. 30 in Section 4.6) by water saturation gravimetry. The samples $D_u$close and $D_u$far are taken from the reimpregnated piece 04.001-OC-D-ri. Fig. 37 shows the variation in porosity as a function of impregnation time for these sub-samples. The porosity value of 0.26 % was found in sub-sample $D_u$close. This represents the residual porosity in *in situ* and laboratory impregnated granodiorite samples. Two reasons exist for the residual porosity: first the volume of polymerized PMMA is about 20 % less than MMA due to shrinking and second the sawing artefacts cause an increase in porosity when preparing the sub-samples. A higher porosity of 0.35 % was detected for sub-sample $D_u$far, which represents only laboratory impregnated granodiorite.

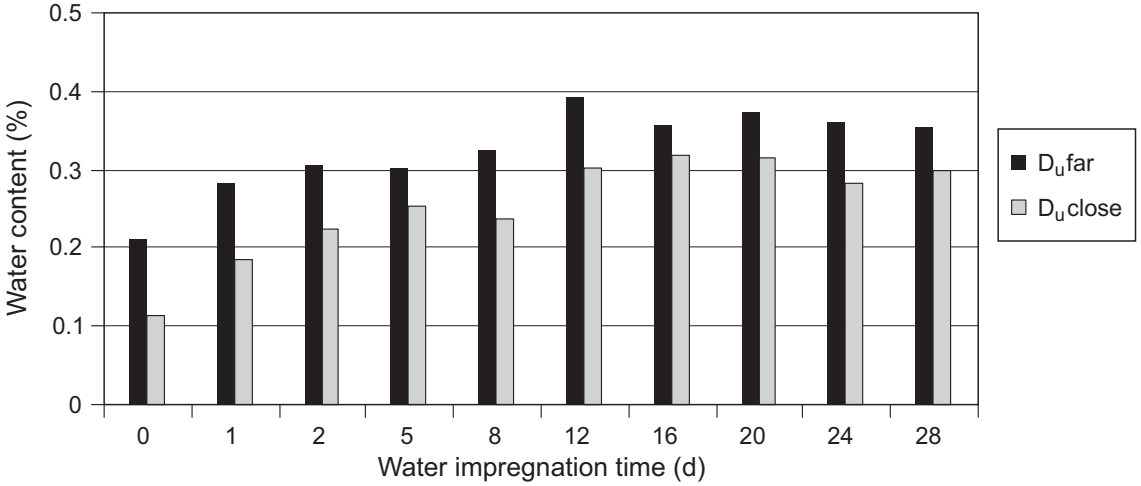

Fig. 37: Variation in porosity as a function of impregnation time for sub-samples $D_u$close and $D_u$far

5.4 Porosity analyses based on thermo gravimetry

The chemical porosimetry (Möri et al. 2003) is based on thermo gravimetry which measures the change in mass as a function of temperature. The mass in crushed granodiorite rock samples decreases when heating the samples up to 420° C when the ^{14}C-MMA in the sample is totally decomposed. Here it is important to notice that the sample sizes varied from 20 to 30 mm^3 in volume (about 60 to 80 mg of crushed rock) in the thermo gravimetry analyses which means one hundred times smaller samples than in water gravimetry and ^{14}C-MMA analyses.

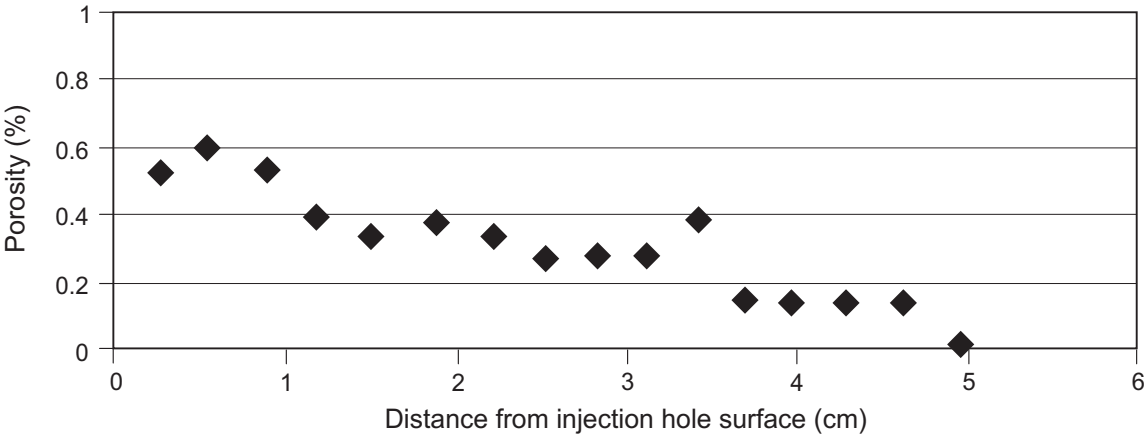

Fig. 38: Result of chemical porosity analyses of *in situ* impregnated sample 04.001-OC-E.

Fig. 38 presents the porosity profile of *in situ* impregnated sub-sample 04.001-OC-E. The profile exceeds a depth of 5 cm from the injection hole surface. A clear decrease in porosity was found indicating poor intrusion of MMA into the granodiorite matrix *in situ* to a depth of 5 cm from the injection hole surface. Fig. 39 shows the porosity profile of sub-sample 04.001-OC-D-ri up to a depth of 10 cm. The porosity in the first detection point which is taken at a depth of 0.2 mm from the injection hole surface is significantly higher than the porosity values in deeper depths. This strengthens the results given by Möri (2005) which states that the borehole disturbed zone in sample 04.001 consists of a 3 mm thick skin where mineral grains are

disturbed and grain boundary pores are widened due to the drilling process leading to enhanced porosity. After this depth the porosity value, which represents the laboratory ^{14}C-MMA porosity, is 0.67±0.07 % being in good agreement with the water saturation porosity of 04.001-IHC samples (0.53 – 0.78 %). Notice that in the chemical porosity analysis results of the sawing artefacts that increase the porosity values are not shown.

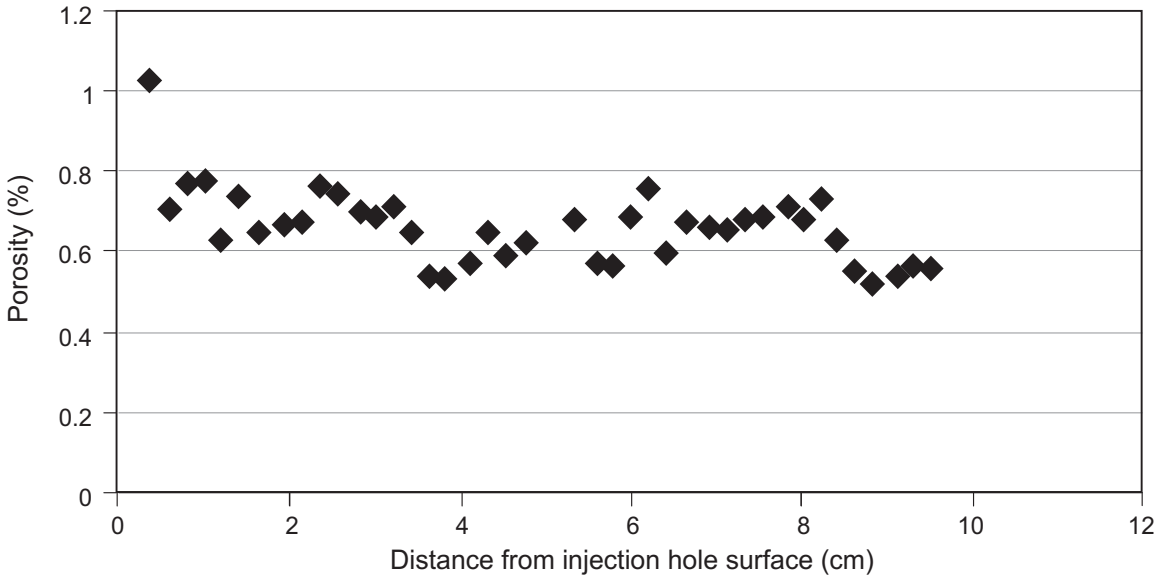

Fig. 39: Result of chemical porosity analyses of *in situ* + laboratory sample 04.001-OC-D-ri

5.5 Mercury porosimetry results

The sawing schemes of 04.001-OC-D-ri sub-samples for mercury porosimetry are presented in Fig. 30. D_uHgC1 and C2 represent the sub-samples taken next to the injection hole surface whereas D_uHg F1 and F2 represent the sub-samples taken at a depth of 7 cm from the injection hole surface. Likewise samples of rock slice 04.001-OC-E (EHgC1, C2, F1 and F2) were taken for mercury porosimetry. The mercury porosimetry results and the diagrams showing incremental intrusion of mercury as a function of pore diameter are listed in Appendix 2. The porosity values are listed in Tab. 9. The sub-samples were sawn by a diamond saw which causes minimal artefacts on the samples. However some increased porosity was found due to sawing by Hellmuth et al. (1995) leading to increase of micrometric aperture pores in pore diameter distribution. The sawing artefacts are emphasized due to the fact that the sample size is only about 2 cm^3 (about 5 g) in mercury porosimetry analyses. This is about ten times smaller sample size than in water and PMMA porosimetry analyses.

Mercury intrusion reveals here the residual porosity of PMMA impregnated samples caused by sawing artefacts, stress relaxation and PMMA shrinking. First the residual porosity for *in situ* and laboratory PMMA impregnated sub-sample (D_uHg C1 and C2) is 0.14 % which is in good agreement with the residual PMMA porosity value caused by a shrinking effect (Siitari-Kauppi, 2002) indicating that all open pore space is filled by MMA in this sub-sample and that sawing artefacts are minimized.

The residual porosity of *in situ* PMMA impregnated sample is 0.35 % which is a reasonable value for the porosity caused by sawing artefacts, stress relaxation and PMMA shrinking. If we compare this value to the *in situ*+laboratory impregnated residual porosity of 0.14 % we could

conclude that stress relaxation effect and sawing artefacts represent about 0.2 % porosity. The residual porosity of the laboratory PMMA impregnated sample is 0.52 %, which is a fairly high value. The porosity of the non-impregnated sample was 0.81 % which is in good agreement with the water saturation porosity values of 0.82 % and 0.85 % given for the same type of samples (see section 5.3, Tab. 8). When comparing this value to the laboratory impregnated porosity value of 0.52 %, we could evaluate that the stress relaxation effect and sawing artefact causes about 0.3 % porosity.

Tab. 9: Mercury porosimetry results (Dr. P Klobes BAM, Germany)

Sample code	**Porosity** (%)	**Porosity** (%) Average of two parallel samples	**Notes**
D_uHg C1 D_uHg C2	0.1280 0.1604	**0.14**	*In situ* + laboratory impregnated 04.001-OC-D-ri Next to injection hole surface
D_uHg F1 D_uHg F2	0.5102 0.5248	**0.52**	Laboratory impregnated 04.001-OC-D-ri 7 cm from injection hole surface
EHg C1 EHg C2	0.3291 0.3695	**0.35**	*In situ* impregnated 04.001-OC-E Next to injection hole surface
EHg F1 EHg F2	0.8035 0.8081	**0.81**	Non impregnated 04.001-OC-E 5 cm from injection hole surface

Tab. 10: Results of water saturation gravimetry and mercury porosimetry for sub-samples from the *in situ* over core PSG 04.001-OC

water saturation gravimetry	
0.6-0.9 %	virgin Grimsel granodiorite, core scale
0.10-0.15 %	porosity after impregnation due to shrinking
0.35 %	*in situ* impregnated sample, close to injection borehole surface
0.7-0.9 %	*in situ* impregnated sample, far from injection borehole surface (=virgin)
mercury porosimetry	
0.7 %	virgin Grimsel granodiorite, core scale
0.12 %	porosity after impregnation due to shrinking
0.32 %	*in situ* impregnated sample, close to injection borehole surface
0.52 - 0.81 %	*in situ* impregnated sample, far from injection borehole surface (=virgin)

6 Conclusions

It was clearly observed that air ventilation drying around the injection borehole was not effective enough to dry the rock matrix when ^{14}C-MMA impregnation was applied *in situ*. However the penetration of ^{14}C-MMA into Grimsel granodiorite *in situ* was successfully tested. Autopolymerisation of the resin reduced the impregnation, but the thermal polymerisation succeeded well. The overcored rock sample was sawn into five slices and their surfaces were autoradiographed. Unfortunately the tracer activity (22 kBq mL^{-1}) was too low to achieve PMMA autoradiographs (film or digital). Part of one slice was re-impregnated in the laboratory to determine the residual porosity of the *in situ* impregnated sample.

The porosity values were determined by water saturation gravimetry, mercury porosimetry and chemical porosity measurement technique based on thermo gravimetry for several sub-samples from the overcore. The real *in situ* porosity was analysed by thermo gravimetry. The amount of PMMA showed clearly a decreasing tendency from injection borehole surface to a depth of 5 cm in the rock matrix. The *in situ* porosity profile could be calculated from the porosity of a re-impregnated sub-sample by PMMA autoradiography. Fig. 40 presents the porosity profiles measured by both above mentioned techniques; the results are in good agreement but it shows clearly the improper intrusion of MMA into the rock which might be due to insufficient drying of open pore space. Tab. 11 presents the experiments and the concluded porosity results.

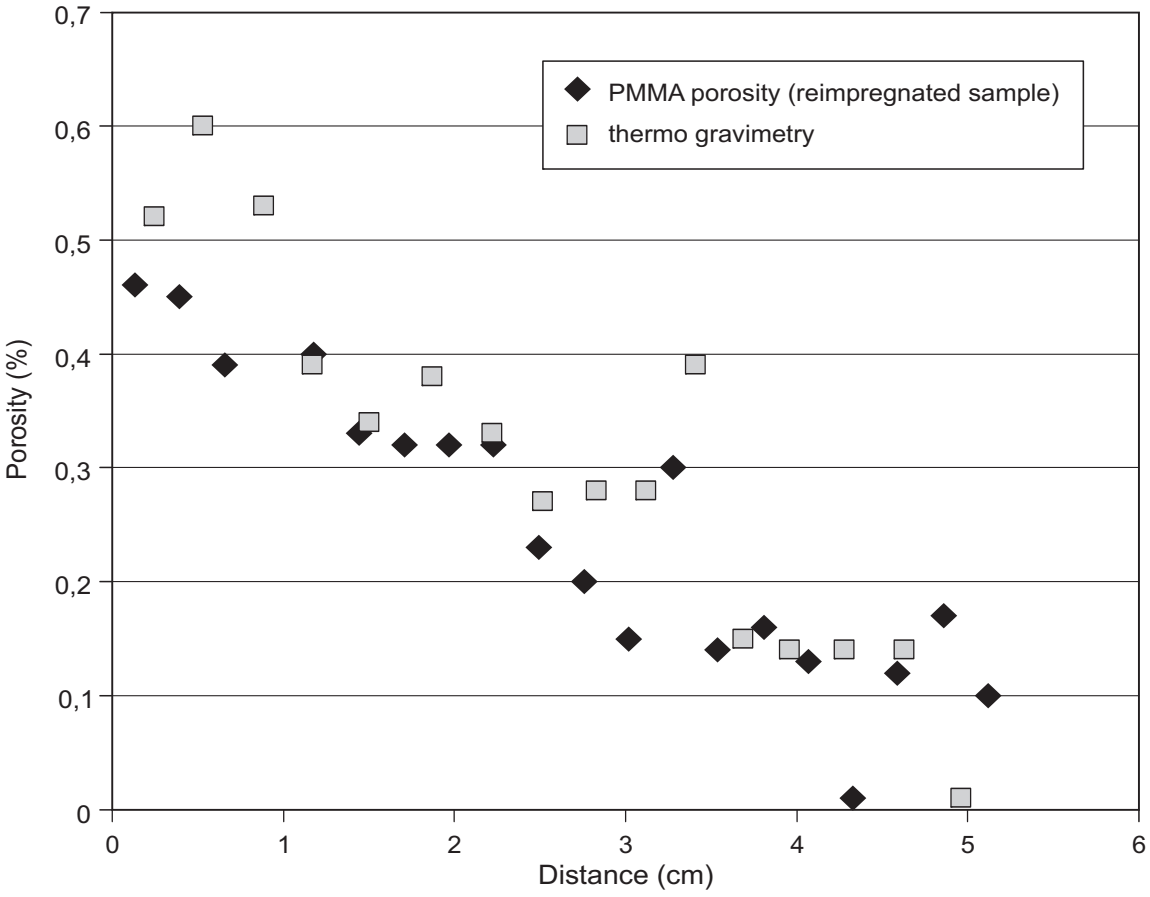

Fig. 40: Residual porosity profile of re-impregnated sub-sample PSG 04.001-OC D

Tab. 11: Experimental procedures of core and in situ test. In addition concluded porosity results are listed

	core scale	***in situ***
rock matrix	Grimsel granodiorite	Grimsel granodiorite
dimensions	length 3 – 11 cm Ø 3 – 7 cm	at a depth of one meter from the tunnel wall
Drying /time	vacuum, aluminium chamber /1 – 2 weeks	air flushing /3 weeks
Impregnation /time	vacuum, aluminium chamber /3 – 14 days	5 bar pressure /36 days
polymerisation	irradiation with ^{60}Co source	heating, chemical initiator
tracer activity	888 kBq mL-1	22 kBq mL-1
analysis	PMMA autoradiography water gravimetry thermo gravimetry Hg porosimetry	UV light detection Re-impregnation /PMMA autoradiography water gravimetry thermo gravimetry Hg porosimetry
depth of penetration	samples fully impregnated	max. 5 cm
porosity determined	0.7 ± 0.2 %	0.4 $\pm$ 0.3 %

The schematic picture of the experiment is shown in Fig. 41; red illustrates the location of the resin in the injection hole, green colour illustrates resin impregnated matrix. An important result from this study is that porosity values were found to be 20 – 30 % lower under *in situ* conditions than porosity values measured in the lab experiments.

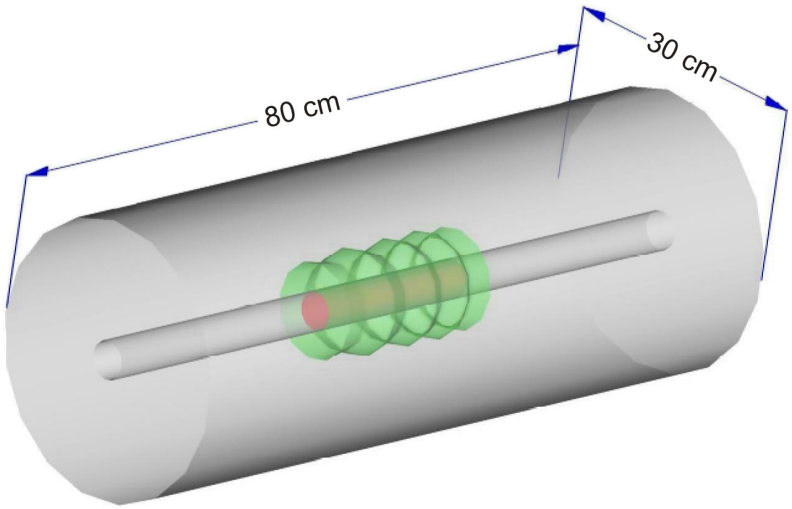

Fig. 41: Schematic diagram of the *in situ* experiment. The red area illustrates the location of methylmethacrylatre in the injection hole, the green colour, the resin impregnated area

7 References

Frieg, B., Alexander, W.R., Dollinger, H., Buhler, C., Haag, P., Möri, A. & Ota, K., (1998): In Situ Resin Impregnation or Investigating Radionuclide Retardation in Fractured Repository Host Rocks, Journal of Contaminant Hydrology 35, 115-130

Hellmuth, K-H., Siitari-Kauppi, M. & Lindberg, A., (1993): Study of porosity and migration pathways in crystalline rock by impregnation with ^{14}C-polymethylmethacrylate, Journal of Contaminant Hydrology 13, 403-418

Hellmuth, K-H., Lukkarinen & S. Siitari-Kauppi, M. (1994): Rock matrix studies with carbon-14-polymethylmethacrylate (PMMA): method development and applications. Isotopenpraxis. Isotopes in Environmental and Health Studies 30, 47-60

Hellmuth, K-H., Klobes, P., Meyer, K., Röhl-Kuhn, B., Siitari-Kauppi, M., Hartikainen, K., Hartikainen, J. & Timonen, J. (1995): Matrix retardation studies: size and structure of the accessable pore space in fresh and altered crystalline rock. Z.geol.Wiss., 23(5/6), 691-706

Kauppi I. (2007): Thermogravimetria, Grimselin Granodioriitin huokoisuusmääritykset. Työraportti 8.2005

Kelokaski, M., Siitari-Kauppi, M., Sardini, P., Möri, A.& Hellmuth, K-H. (2006): Characterisation of pore space geometry by ^{14}C-MMA impregnation-Development work for in situ studies. Journal of Geochemical Exploration Vol. 90, issues 1-2, 45-52

Kämäräinen, E.-L., Haaparanta, M., Siitari-Kauppi, M., Koivula, T., Lipponen, T. & Solin, O. (2006): Analysis of ^{18}F-labelled synthesis products on TLC plates: comparison of radioactivity scanning, film autoradiography, and a phosphoimaging technique. Applied Radiation and Isotopes 64. 1043-1047

McKinley, I.G. (1989): Applying natural analogues in predictive performance assessment: 1. Principles and requirements, 2. Examples and discussions. In: Risk analysis in nuclear waste management. Klewer, Academic, Publ., Dordrecht, The Netherlands

Möri, A. (2006): Personal communication

Möri, A. (2005): GTS Phase VI-Pore Space geometry (PSG) Experiment-In situ impregnation of matrix pores in granite rock – Study of a potential borehole disturbed zone (BDZ), Arbeitsbericht NAB 05-19

Möri A.; Mazurek, M.; Adler, M.; Schild, M., Siegesmund, S.; Vollbrecht, A.; Ota, K.; Ando, T.; Alexander, W.R.; Smith, P.A.; Haag, P. & Buehler, Ch. (2003): Grimsel Test Site Investigation Phase IV (1994-1996): The Nagra-JNC *in situ* study of safety relevant radionuclide retardation in fractured crystalline rock IV: The *in situ* study of matrix porosity in the vicinity of a water conducting fracture. Nagra Technical Report NTB 00-08. Nagra, Wettingen

Ota, K., Alexander, W.R., Smith, P.A., Möri, A., Frieg, B., Frick, U.,Umeki, H., Amano, K., Cowper, M.M. & Berry, J.A. (2001): Building confidence in radionuclide transport models for fractured rock: the Nagra/JNC radionuclide retardation programme. In: Hart, K.P., Lumpkin, G.R. (Eds.), Scientific Basis for Nuclear Waste Management XXIV, Mater. Res. Soc. Symp. Proc., vol. 663, pp. 1033–1041

Pinnioja, S., Siitari-Kauppi, M., & Lindberg, A. (1999): Effect of feldspar composition on thermoluminescence of minerals separated from food. Radiation Physics Chemistry, 54, 505–516

Sardini, P., Siitari-Kauppi, M., Beaufort, D. & Hellmuth, K-H (2006): On the connected porosity of mineral aggregates in crystalline rocks. American Mineralogist 91, 1069-1080

Siitari-Kauppi, M., Flitsiyan, E. S., Klobes, P, Meyer, K. & Hellmuth, K.-H. (1998): Progress in physical rock matrix characterization: structure of the pore space. In: I.G. McKinley, C. McCombie (edits.), Scientific Basis for Nuclear Waste Management XXI, Mat. Res. Soc. Symp. Proc. 506, 671-678

Siitari-Kauppi, M. (2002): Development of ^{14}C-polymethylmethacrylate method for the characterisation of low porosity media. Application to rocks in geological barriers of nuclear waste storage. Academic Dissertation. Report Series in Radiochemistry 17/2002

Vomvoris, S., Frieg, B. (eds.), Bossart, P., Gmünder, C., Heiniger, P., Jaquet, O. & Watanabe, P. (1992): Grimsel Test Site: Overview of Nagra field and modeling activities in the Ventilation Drift (1988-1990). Nagra Technical Report NTB 91-34. Nagra, Wettingen

Acknowledgments

"The authors would like to extend their thanks to the many colleagues who contributed to this work in some capacity or another, especially thanks to Dr. Peter Klobes from the Bundesanstalt für Materialforschung und -prüfung (BAM), Berlin Germany who performed the Hg porosity measurements. We would like to thank the Ministry of Trade and Industry (MIT) of Finland which financed the work under project cluster KYT2010."

Appendix 1

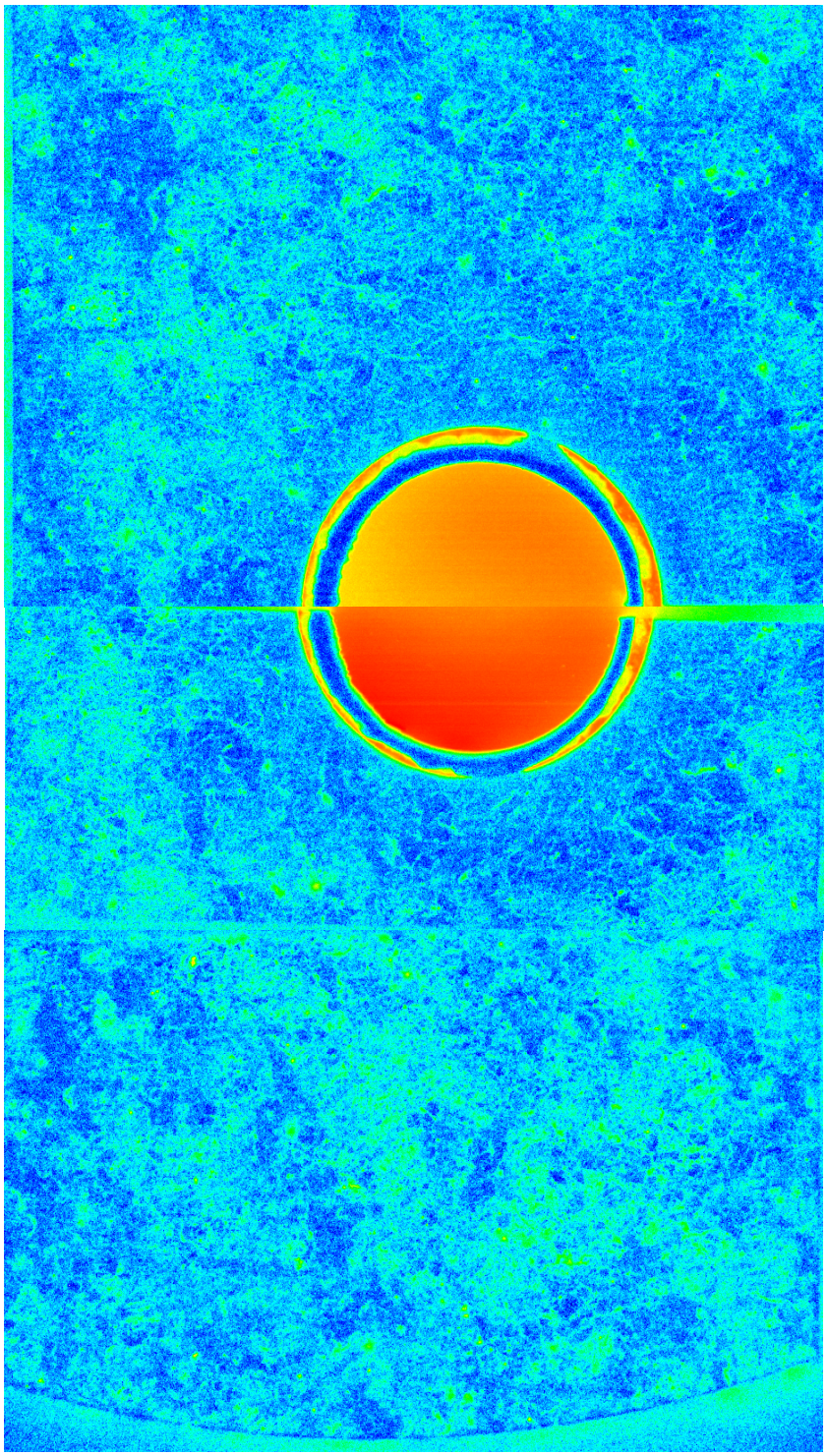

D 3/A

D 2/A

D 1/A

FLA scanner analysis of re-impregnated sample PSG 04.001-OC D. Surface A was exposed on an IP plate for 20 hours. Different shades of blue colour on the FLA image represent different porosities; dark blue shows areas that have about 0.1 – 0.2 % porosities whereas light blue presents about 0.5 – 0.6 % porosities.

Appendix 2 (1)

04.001-OC-D-ri and 04.001-OC-E sub-sample mercury porosimetry results

D_uHg C1

```
Intrusion Data Summary
(From Pressure 0.0007 to 420.0000 MPa)
Total Intrusion Volume = 0.0005 mL/g
Total Pore Area = 0.004 m²/g
Median Pore Diameter (Volume) = 120628.3 nm
Median Pore Diameter (Area) = 27.3 nm
Average Pore Diameter (4V/A) = 451.9 nm
Bulk Density = 2.6902 g/mL
Apparent (skeletal) Density = 2.6937 g/mL
Porosity = 0.1280 %
Stem Volume Used = 1 % ****
```

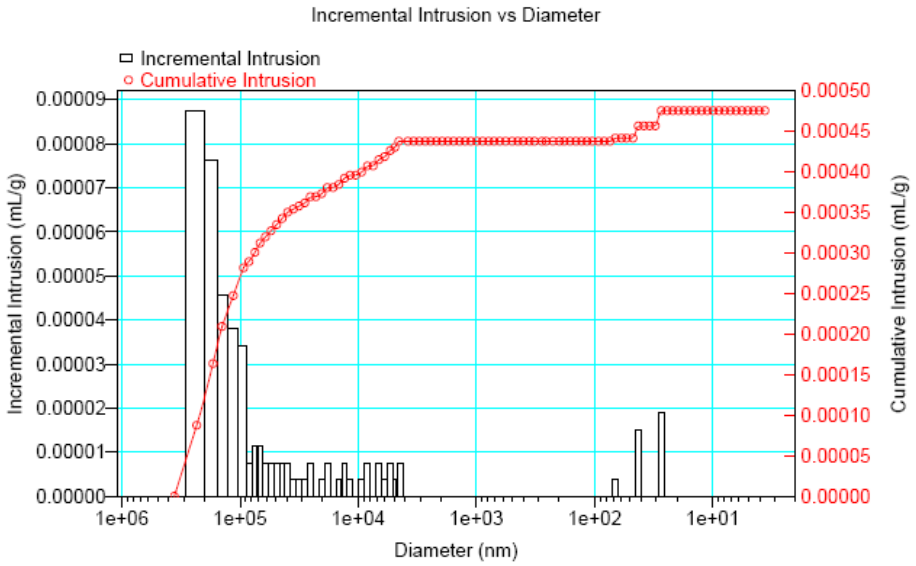

D_uHg C2

```
Intrusion Data Summary
(From Pressure 0.0007 to 420.0000 MPa)
Total Intrusion Volume = 0.0006 mL/g
Total Pore Area = 0.003 m²/g
Median Pore Diameter (Volume) = 119479.4 nm
Median Pore Diameter (Area) = 136.0 nm
Average Pore Diameter (4V/A) = 827.1 nm
Bulk Density = 2.6807 g/mL
Apparent (skeletal) Density = 2.6850 g/mL
Porosity = 0.1604 %
Stem Volume Used = 1 % ****
```

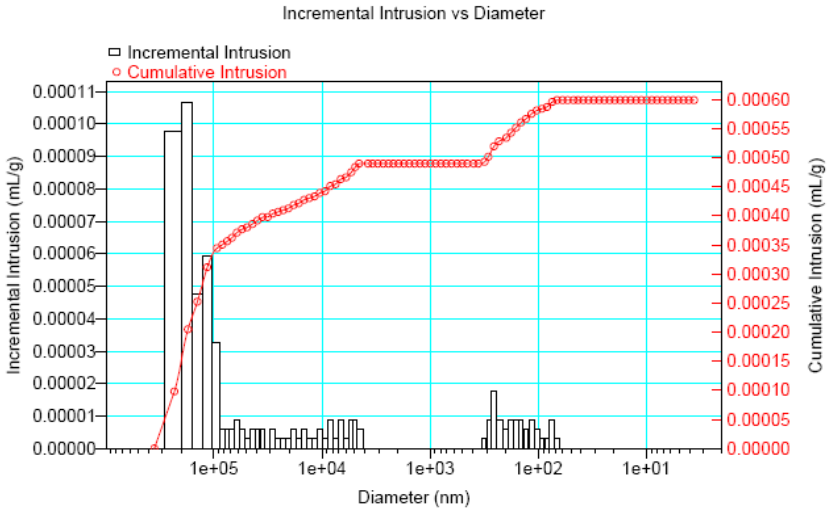

Appendix 2 (2)

D_uHg F1

```
Intrusion Data Summary
(From Pressure 0.0007 to 420.0000 MPa)
Total Intrusion Volume = 0.0019 mL/g
Total Pore Area = 0.016 m²/g
Median Pore Diameter (Volume) = 122849.8 nm
Median Pore Diameter (Area) = 117.0 nm
Average Pore Diameter (4V/A) = 479.7 nm
Bulk Density = 2.6693 g/mL
Apparent (skeletal) Density = 2.6830 g/mL
Porosity = 0.5102 %
Stem Volume Used = 3 % ****
```

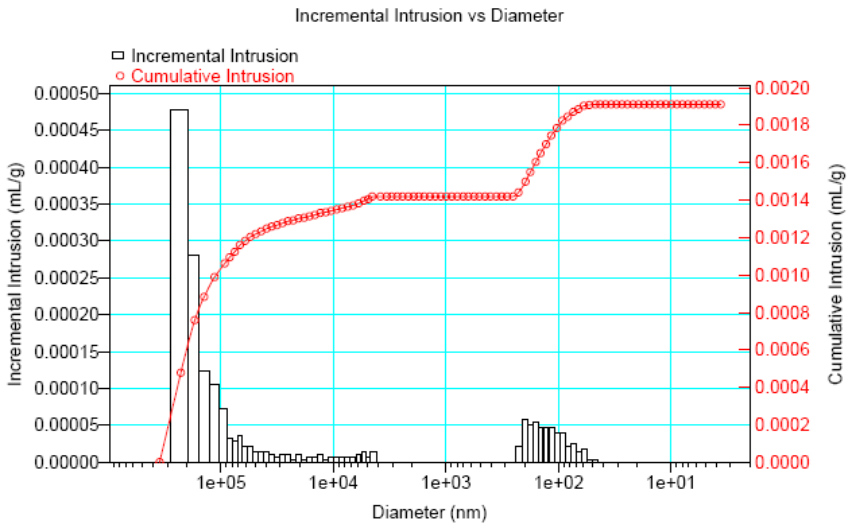

D_uHg F2

```
Intrusion Data Summary
(From Pressure 0.0007 to 420.0000 MPa)
Total Intrusion Volume = 0.0019 mL/g
Total Pore Area = 0.027 m²/g
Median Pore Diameter (Volume) = 140603.8 nm
Median Pore Diameter (Area) = 42.9 nm
Average Pore Diameter (4V/A) = 292.1 nm
Bulk Density = 2.7059 g/mL
Apparent (skeletal) Density = 2.7201 g/mL
Porosity = 0.5248 %
Stem Volume Used = 2 % ****
```

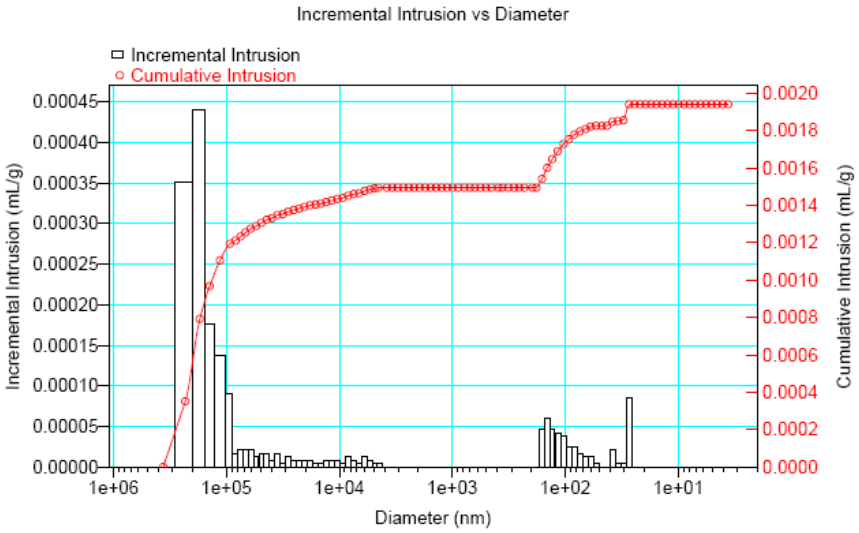

Appendix 2 (3)

EHgC1

```
Intrusion Data Summary
(From Pressure 0.0007 to 420.0000 MPa)
Total Intrusion Volume = 0.0012 mL/g
Total Pore Area = 0.043 m²/g
Median Pore Diameter (Volume) = 168.2 nm
Median Pore Diameter (Area) = 61.0 nm
Average Pore Diameter (4V/A) = 116.1 nm
Bulk Density = 2.6625 g/mL
Apparent (skeletal) Density = 2.6713 g/mL
Porosity = 0.3291 %
Stem Volume Used = 2 % ****
```

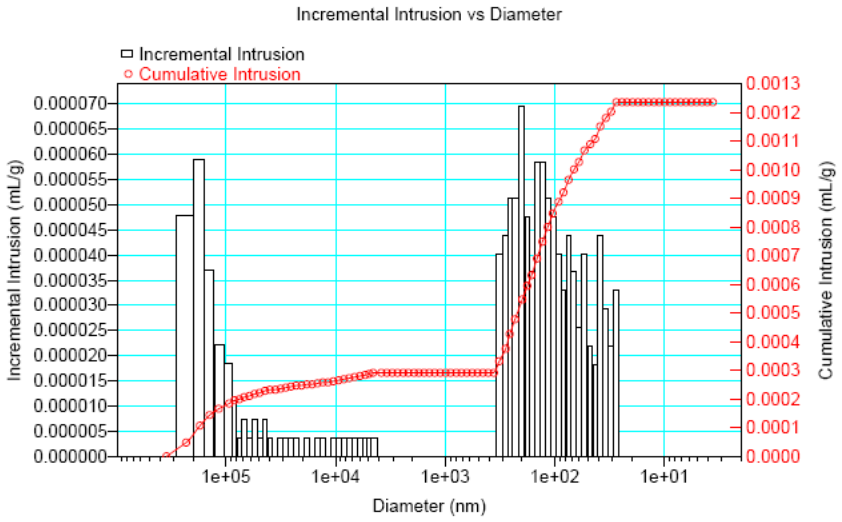

EHg C2

```
Intrusion Data Summary
(From Pressure 0.0007 to 420.0000 MPa)
Total Intrusion Volume = 0.0014 mL/g
Total Pore Area = 0.025 m²/g
Median Pore Diameter (Volume) = 309.1 nm
Median Pore Diameter (Area) = 103.4 nm
Average Pore Diameter (4V/A) = 219.9 nm
Bulk Density = 2.6629 g/mL
Apparent (skeletal) Density = 2.6728 g/mL
Porosity = 0.3695 %
Stem Volume Used = 2 % ****
```

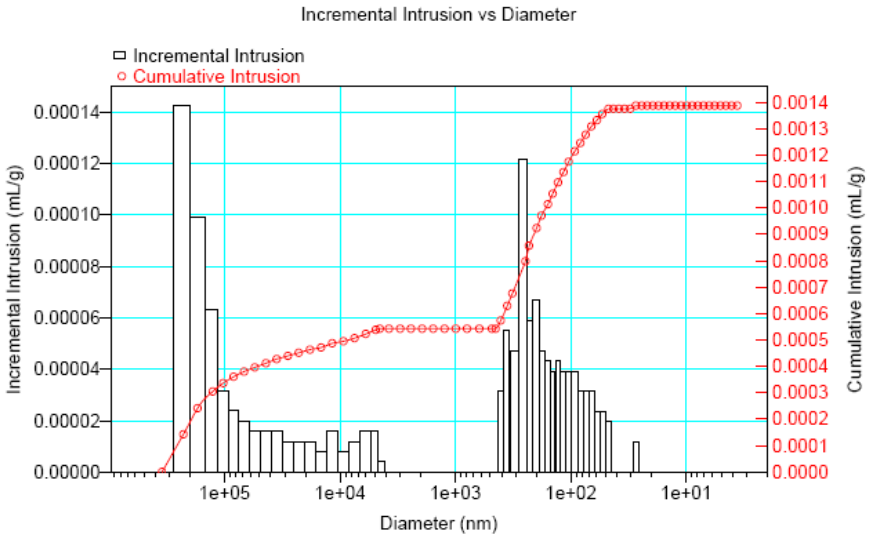

Appendix 2 (4)

EHg F1

```
Intrusion Data Summary
(From Pressure 0.0007 to 420.0000 MPa)
Total Intrusion Volume = 0.0030 mL/g
Total Pore Area = 0.063 m²/g
Median Pore Diameter (Volume) = 554.3 nm
Median Pore Diameter (Area) = 45.9 nm
Average Pore Diameter (4V/A) = 189.3 nm
Bulk Density = 2.6826 g/mL
Apparent (skeletal) Density = 2.7043 g/mL
Porosity = 0.8035 %
Stem Volume Used = 4 % ****
```

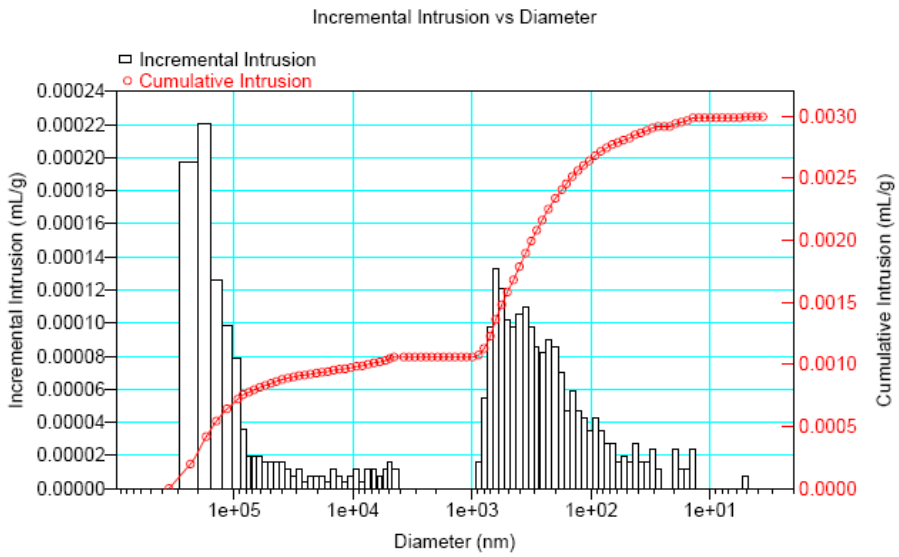

Intrusion Data Summary
(From Pressure 0.0007 to 420.0000 MPa)
Total Intrusion Volume = 0.0030 mL/g
Total Pore Area = 0.053 m²/g
Median Pore Diameter (Volume) = 541.6 nm
Median Pore Diameter (Area) = 76.1 nm
Average Pore Diameter (4V/A) = 227.8 nm
Bulk Density = 2.6626 g/mL
Apparent (skeletal) Density = 2.6843 g/mL
Porosity = 0.8081 %
Stem Volume Used = 4 % ****